

## **PPAR $\beta$ stimulation induces rapid cardiac growth and angiogenesis via direct activation of calcineurin**

Nicole Wagner<sup>1,2</sup>, Chantal Jehl-Piétri<sup>1,2</sup>, Pascal Lopez<sup>1,2</sup>, Joseph Murdaca<sup>1,2</sup>, Christian Giordano<sup>1,2</sup>, Chantal Schwartz<sup>1,2</sup>, Pierre Gounon<sup>3</sup>, Stéphane N. Hatem<sup>4,5</sup>, Paul Grimaldi<sup>1,2</sup>, Kay-Dietrich Wagner<sup>1,2</sup>

<sup>1</sup>INSERM U907, 06107 Nice, France, <sup>2</sup>Université de Nice-Sophia Antipolis, 06108 Nice, France, <sup>3</sup>Service de Microscopie Electronique Université de Nice-Sophia Antipolis, 06108 Nice, France, <sup>4</sup>INSERM, UMR S621, Paris, 75013 France; <sup>5</sup>Université Pierre et Marie Curie-Paris 6, UMR S621, Paris, 75013 France

**Running title:** Rapid response to PPAR $\beta$  activation in the heart

**Word count:** 6496

Address for correspondence:

Paul Grimaldi  
INSERM U907  
28, Avenue Valombrose  
06107 Nice, France  
Phone : +33 493 81 84 96  
Fax: +33 493 81 54 32  
e-mail: paul.grimaldi@unice.fr

Kay-Dietrich Wagner  
INSERM U907  
28, Avenue Valombrose  
06107 Nice, France  
Phone : +33 493 81 84 98  
Fax: +33 493 81 54 32  
e-mail: kwagner@unice.fr

**Abstract**

**Aims:** Peroxisome proliferator-activated receptors (PPARs) are ligand-activated transcription factors. PPAR $\beta$  agonists were suggested as potential drugs for the treatment of metabolic syndrome, but effects of PPAR $\beta$  activation on cardiac growth and vascularisation are unknown. Thus, we investigated the consequences of pharmacological PPAR $\beta$  activation on the heart and the underlying molecular mechanisms.

**Methods:** Male C57/Bl6 mice were injected with the specific PPAR $\beta$  agonists GW0742 or GW501516, or vehicle for different time points and cardiomyocyte size and vascularisation determined. Expression differences were investigated by quantitative RT-PCR and Western Blotting. In addition, the effects of PPAR $\beta$  stimulation were compared to hearts of mice undergoing long-term voluntary exercise or pharmacological PPAR $\alpha$  activation.

**Results:** Already after 5 hours of GW0742 injection, we detected an enhanced angiogenesis compared to vehicle-injected controls. After 24 hours, the heart to body weight ratios were higher in mice injected with either GW0742 or GW501516 vs. controls. The increased heart size was due to cardiomyocyte enlargement. No signs of pathological cardiac hypertrophy (i.e. apoptosis, fibrosis, or deteriorated cardiac function) could be detected. The effects are mediated via calcineurin A (CnA) activation as: I) CnA was upregulated, II) GW0742 administration or co-transfection of PPAR $\beta$  significantly stimulated the activity of the CnA promoter, III) PPAR $\beta$  protein bound directly to the CnA promoter, IV) the calcineurin A target genes NFATc3, Hif-1 $\alpha$ , and Cdk 9 were upregulated in response to PPAR $\beta$  stimulation, and V) inhibition of CnA activity by cyclosporine A abolished the hypertrophic and angiogenic responses to PPAR $\beta$  stimulation. **Conclusion:** Our data suggest PPAR $\beta$  pharmacological activation as a novel approach to increase cardiac vascularisation and cardiac muscle mass.

**Key words:** Angiogenesis, Calcineurin, Gene transcription, Hypertrophy, Peroxisome proliferator-activated receptor

## Introduction

Peroxisome proliferator-activated receptors (PPARs) are ligand-activated transcription factors<sup>1</sup>. They have become in focus as targets for the treatment of glucose and lipid abnormalities<sup>2-4</sup>. PPARs are members of the nuclear receptor superfamily. They exist in three isoforms, PPAR $\alpha$ , PPAR $\beta$  (formerly PPAR $\delta$ ), and PPAR $\gamma$ . All PPARs form heterodimers with retinoid X receptors, and upon ligand binding, use the basal transcriptional machinery to augment gene expression<sup>5</sup>. Via this mechanism, PPARs regulate lipoprotein and glucose metabolism, and modulate adipose tissue, liver, endothelium, and skeletal muscle phenotypes. Synthetic PPAR $\alpha$  and PPAR $\gamma$  agonists are already in clinical use for the treatment of hyperlipidemia and type 2 diabetes, respectively (reviewed in 6).

More recently, PPAR $\beta$  activation became in focus as an interesting novel approach for the treatment of metabolic syndrome and associated cardiovascular diseases<sup>7,8</sup>. Using pharmacological stimulation and transgenic animal models, it has been shown that PPAR $\beta$  activation increases oxidative metabolism, insulin responsiveness, fatty acid burning<sup>9,10</sup>, and induces a fibre type transition in skeletal muscle<sup>11</sup>. Furthermore, PPAR $\beta$  activation reduces fat mass, normalizes adipokine secretion, and insulin responsiveness in adipose tissue<sup>12</sup>. Thus, PPAR $\beta$  activation mimics the beneficial effects of physical exercise. For the heart, it has been shown that PPAR $\beta$  activation stimulates fatty acid oxidation<sup>13</sup>, has anti-inflammatory effects on the vascular system<sup>14</sup> and reduces ischemia/reperfusion-induced injury in transgenic mice<sup>15</sup>. Whether pharmacological specific PPAR $\beta$  activation acts on the heart *in vivo* and how these potential effects are mediated in molecular terms remained to be elucidated.

We show here that specific PPAR $\beta$  stimulation rapidly induces cardiac angiogenesis and myocyte growth and that these effects are mediated at least in part by direct transcriptional activation of calcineurin.

## Methods

### *Animals*

The investigation conforms with the *Guide for the Care and Use of Laboratory Animals* published by the US National Institutes of Health (NIH Publication No. 85-23, revised 1996). Experiments were approved by the University of Nice Animal Care and Use Committee.

10 weeks old male C57/BL6J (Janvier, France) mice were subcutaneously injected with GW0742 (Glaxo Smith Kline) or GW501516 (Alexis Biochemicals) dissolved in DMSO at 1mg/kg once daily (2pm) according to the duration of treatment (24, 48, 96 hrs). Controls received DMSO injections. Cyclosporine A (Sigma) dissolved in DMSO was administered daily (9am) by subcutaneous injection in a dose of 20mg/kg. Clofibrilic acid (Sigma) was injected one time a day (2pm) in a dose of 300mg/kg. Propranolol (Sigma) dissolved in PBS was injected subcutaneously in a dose of 0.5mg/kg. Physical training was performed by keeping the animals in cages for voluntary physical exercise (Techniplast, Italy) equipped with a running wheel (25 cm diameter) for five weeks.

### *Histological and immunohistochemical analysis*

Paraffin sections (5µm) were stained with hematoxylin and eosin. Mean cardiomyocyte diameters were determined by a blinded investigator measuring at least 30 cells per heart of four hearts for each condition. Collagen-specific Sirius Red (Waldeck GmbH, Münster, Germany) staining for measurement of interstitial fibrosis was performed according to manufacturer's instructions. Antibodies, dilutions and kits used for immunohistochemistry are described in supplementary methods. Slides were viewed under an epifluorescence microscope connected to a digital camera with the Spot software (Universal Imaging Corp.).

*TUNEL-labelling of apoptotic cells*

Apoptotic cells were detected by TUNEL staining in paraffin-embedded heart sections using the In situ Cell Death Detection Kit (Roche Molecular Biochemicals) as described previously<sup>16</sup>. TUNEL-positive cells/field were counted. Five tissue sections were analysed from 3 different controls and 3 hearts each at different time points of GW0742 treatment or physical exercise for five weeks. Heart sections of mice with hereditary cardiomyopathy due to injection of miR 1 in the oocyte<sup>16</sup> served as a positive control.

*SDS-Page and Western Blot*

Total heart lysates from the mice treated with GW0742 or vehicle alone (DMSO) were prepared, electrophoresed, and blotted as described<sup>16</sup>. Subcellular fractionation of heart tissues was performed using the Qproteome™ Cell Compartment Kit (Quiagen) according to manufacturer's instructions. Antibodies for immunodetection are mentioned in supplementary methods.

*Electron microscopy*

For ultrastructural analysis of cardiac muscle, small pieces were fixed in 1.6% glutaraldehyde in 0.1M phosphate buffer (pH 7.5), then washed with 0.1M cacodylate buffer (pH 7.5), and post-fixed with 1% osmium tetroxide in the same buffer. Samples were embedded in epoxy resin. Thin sections were contrasted with uranyl acetate and lead citrate and observed with a Philips CM12 electron microscope fitted with a CCD camera (Morada, Olympus SIS).

*Cell culture and transient transfection experiments*

Neonatal mouse cardiomyocytes were isolated as described<sup>17</sup> with minor modifications mentioned in supplementary methods. Adult cardiomyocytes were isolated using the Adumyts kit (Cellutron) according to manufacturers instructions. Adult cardiomyocytes were maintained for 24 hours in serum free medium in the presence of 200nM GW0742 or vehicle. To investigate the effect of PPAR $\beta$  expression on calcineurin promoter activity, a 2.3 kb fragment of the calcineurin promoter in the pGl3basic luciferase expression vector<sup>18</sup> was co-transfected with PPAR $\beta$  and RxR expression constructs<sup>19</sup>. Alternatively, the CnA $\beta$  promoter construct was co-transfected only with the  $\beta$ -galactosidase reporter plasmid and the cells cultured for 48 hours in the presence of 100nM GW0742 or vehicle in the presence or absence of a dominant negative PPAR $\beta$  isoform<sup>19</sup>. Transient co-transfections and assays for luciferase-and  $\beta$ -galactosidase activity are described elsewhere<sup>20</sup>. The putative PPAR responsive element (position -1249bp - -1224bp of the published promoter) was deleted from the CnA $\beta$  promoter construct using the Quik Change II site directed mutagenesis kit (Stratagene). Details are provided in supplementary methods.

*Chromatin immunoprecipitation assay*

Chromatin immunoprecipitation (ChIP) assay was performed on neonatal cardiomyocytes using manufacturers instructions (Upstate). Antibodies and primer sequences are described in supplementary methods.

*Electrophoretic mobility shift assays*

The putative PPAR responsive element from the CnA $\beta$  promoter contained the following sequence: 5'-TTGGCCCCTGAACCATTCAACACTGC-3'. The PPAR responsive element from the acyl-CoA oxidase gene (5'-

CCCGAACGTGACCTTTGTCCTGGTCC-3') served as positive control. Annealed oligonucleotides were <sup>32</sup>P-end labelled in a T4 polynucleotide kinase reaction (New England Biolabs). PPAR $\beta$  and RxR $\alpha$  proteins were generated from full-length cDNAs in pSG5 vector (Stratagene) using the coupled TNT in-vitro-transcription-translation system (Promega). For supershift assays, the identical antibodies as for the CHIP experiments were used. Details are described in supplementary methods.

#### *Quantitative RT-PCR*

Reverse transcriptase polymerase chain reaction (RT-PCR) was performed with 2  $\mu$ g of total RNA as described<sup>16</sup>. Primers for quantitative RT-PCR are listed in supplementary methods.

#### *Echocardiography*

Echocardiography was performed on lightly anesthetized (1% isoflurane in oxygen) mice with a GE Medical System VIVI7 device equipped with an 8- to 14-MHz phased array transducer. The left ventricle (LV) was imaged in parasternal long-axis view to obtain measurements of the LV in time-motion mode. The following measurements were performed: LV end-diastolic diameter (mm/g), interventricular septum diastolic thickness (mm/g), LV posterior wall diastolic thickness (mm/g), and shortening fraction (%). Aortic outflow was estimated by measuring the pulse-wave Doppler velocity in the LV at the level of the aortic annulus and using the following equation:  $\Pi d^2/4 * VTI * HR$ , d is the diameter of the aortic annulus, VTI is the velocity time integral, HR is the heart rate.

*Statistics*

Data are expressed as means  $\pm$  S.E.M. ANOVA with the Bonferroni test as post hoc test was used vs. control. Differences between two groups were tested using the Mann-Whitney test for non-parametric samples. A p-value less than 0.05 was considered statistically significant.

## Results

### *PPAR $\beta$ activation results in a rapid induction of cardiac growth without pathological aspects*

Wild-type mice (C57/BL6J strain) were treated by subcutaneous injection with the specific PPAR $\beta$  agonist GW0742. The animals showed already 24 hours after injection of the specific PPAR $\beta$  agonist an increased heart size when compared to vehicle-injected controls (Figure 1A). Heart weights were significantly higher in mice treated with GW0742 for 24 and 48 hours (Figure 1B) whereas body weights remained unchanged (Figure 1C). Histological analysis revealed a marked increase in cardiomyocyte diameters already 24 hours after GW0742 injection (Figure 1D-F) with a shift of the cardiomyocyte diameter distribution to higher values. This was even more pronounced 48 hours after GW0742 treatment (Figure 1F). The cardiac growth-promoting effect of PPAR $\beta$  stimulation was evident regardless if the animals were treated for 24, 48, (Figure 1A, B, D, E) or 96 hours (Figure 2A, B, C) with GW0742. Five hours after GW0742 injection, this effect was not yet detectable (Figure 1B, D, E, F). Echocardiographic examination in anaesthetized animals confirmed the growth-promoting effect, which is indicated by an increased septum thickness after GW0742 treatment (Figure 1G, a). Interestingly, no functional disadvantages could be detected after PPAR $\beta$  stimulation, i.e. aortic outflow, the ventricular shortening fraction, and left ventricular end-diastolic diameters were completely normal (Figure 1G, b, c, d). Cardiac hypertrophy was still present 10 days after the end of a 48h-treatment, but heart-to-body weight ratios and cardiomyocyte diameters returned to control values 4 weeks after the end of treatment (Figure 2A-C). The degree of cardiac hypertrophy induced by short-term PPAR $\beta$  stimulation was comparable to that achieved by long-term voluntary exercise (training) for 5 weeks (Figure 2A-C). Also on the ultrastructural level, short-term PPAR $\beta$  stimulation resembled the long-term training effect with addition of sarcomeres, dense mitochondrial cristae, normal sarcomere lengths, and no signs of cardiomyocyte damage or fibrosis (Figure 2D). As

qualitative measure for collagen accumulation, we performed Sirius Red staining of cardiac sections. Sirius Red staining showed a decrease in collagen accumulation after long-term training or PPAR $\beta$  stimulation (Figure 2E, F). TUNEL labelling as a marker for DNA damage or repair, which is increased in human and mouse pathological hypertrophy<sup>16, 21</sup>, was not evident after PPAR $\beta$  activation or long-term moderate exercise (Figure 2G, H). Our recently established mouse model for cardiomyopathy<sup>16</sup>, which is due to a miR-1-induced paramutation and characterised by ultrastructural signs of hypertrophic cardiomyopathy and a large number of apoptotic cardiomyocytes, served as a positive control (Figure 2G, He).

The growth-promoting effect seems to be specific for the heart as kidney weights relative to body weights showed no significant differences (data not shown). Furthermore, histological analysis of different organs (i.e. kidney and liver) showed no obvious abnormalities (Figure 1H). No increase in cell size was observed in kidney or liver.

#### *PPAR $\beta$ activation induces rapid cardiac angiogenesis*

Next, we analysed a potential cardiac angiogenic response to PPAR $\beta$  stimulation. Expression of hypoxia-inducible factor 1 $\alpha$  (Hif-1 $\alpha$ ), a well-known inducer of angiogenesis<sup>22</sup>, was already increased after 5 hours and more pronounced after 24 hours (Figure 3A, B). PECAM-1 (CD31) as a marker for newly forming vessels was augmented within the same time- frame after PPAR $\beta$  stimulation (Figure 3B, C). This pro-angiogenic effect of PPAR $\beta$  was also demonstrated by a higher number of BrdU positive cells in the cardiac vasculature of GW0742 treated animals, whereas no difference in the number of BrdU-positive cardiomyocytes or fibroblasts was observed (data not shown). Quantification of isolectin B4-positive vessels confirmed an increased capillary density already after 5 and 24 hours, indicating that angiogenesis precedes cardiomyocyte growth in response to PPAR $\beta$  activation (Figure 3D). Ten days after the end of 48hrs GW0742 treatment, the number of isolectin B4-

positive vessels was not significantly different from the controls anymore (data not shown). Although angiogenesis preceded cardiomyocyte hypertrophy after pharmacological PPAR $\beta$  stimulation, it seems not to be a pre-requisite for cardiomyocyte growth, because GW0742 increased cell diameters and lengths also in isolated adult mouse cardiomyocytes after 24 hours of treatment (Supplementary Figure 1).

The observed cardiac growth and angiogenesis seem to be specific for PPAR $\beta$  activation, as treatment with GW501516, another PPAR $\beta$  agonist, induced exactly the same cardiac phenotype as GW0742 after 24 hours of treatment (Supplementary Figure 2). In contrast, administration of the PPAR $\alpha$  agonist clofibrate, a derivative of fenofibrate, which is in wide clinical use for the treatment of metabolic syndrome<sup>2</sup>, neither led to enhanced cardiac growth nor angiogenesis in a similar short time frame (Supplementary Figure 3).

To investigate whether adrenergic signalling might be involved in GW0742-induced cardiac growth, we performed additional GW0742 treatment experiments in mice in the presence of  $\beta$ -adrenergic blockade using propranolol<sup>23</sup>. Co-administration of propranolol did neither affect the cardiac growth promoting nor the pro-angiogenic responses to PPAR $\beta$  stimulation (Supplementary Figure 4).

#### *PPAR $\beta$ -induced cardiac growth is accompanied by an increased calcineurin expression*

As molecular markers and inducers of cardiac growth, expression of  $\alpha$ - and  $\beta$ - myosin heavy chains (myh6 and myh7, respectively) was only transiently increased, angiotensinogen expression was not significantly changed, whereas atrial natriuretic factor and calcineurin became up-regulated after 5 hours and remained elevated for 96 hours of GW0742 treatment (Figure 4A). Pharmacological PPAR $\beta$  stimulation slightly increased calcineurin protein expression already after 5 hours, which became more pronounced after 24 and 48 hours, whereas PPAR $\beta$  and tubulin protein expression were not altered (Figure 4B). Whether

increased calcineurin protein expression was preceded by calcineurin activation, we were not able to measure directly. Calcineurin activation results in dephosphorylation and subsequent nuclear translocation of NFAT (for review see 24). The enhanced nuclear NFATc3 localization after 5 hours of GW0742 injection (Figure 4C) suggests calcineurin activation happens already earlier. Using subcellular protein fractionation, increased nuclear NFATc3 localization could be determined quantitatively after 5 and 24 hours of GW0742 injection (Figure 4D). In agreement with a described regulation of HIF-1 and Cdk9 by calcineurin<sup>25,26</sup>, we detected enhanced Hif-1 $\alpha$  (Figures 3A, 4D) and Cdk9 protein (Figure 4E) expression already after 5 hours of PPAR $\beta$  stimulation, which might contribute to enhanced angiogenesis and cardiac growth.

To exclude the possibility that GW0742 directly affects the mRNA or protein stability of calcineurin and Hif-1, we cultured neonatal cardiomyocytes and inhibited transcription or translation using actinomycin D and cycloheximide, respectively. GW0742 treatment showed no significant effects on calcineurin and Hif-1 $\alpha$  mRNA stability (Supplementary Figure 5). Calcineurin protein stability was also not significantly altered by GW0742 in neonatal cardiomyocytes *in vitro*. Hif-1 $\alpha$  protein was barely detectable in the cultured cells and disappeared completely upon cycloheximide treatment, independently on the presence of GW0742 in the culture medium (Supplementary Figure 5).

#### *PPAR $\beta$ directly activates calcineurin*

To test whether PPAR $\beta$  could directly regulate calcineurin expression, we performed immunohistological double- labelling and show that both proteins are co-expressed in adult mouse hearts *in vivo* (Figure 5A, a, b) and in isolated neonatal cardiomyocyte cultures *in vitro* (Figure 5A, c, d). Addition of 200nM GW0742 significantly stimulated the activity of the published CnA $\beta$  promoter<sup>18</sup> in neonatal cardiomyocyte cultures (Figure 5B). Retroviral

transduction of neonatal cardiomyocyte cultures with a dominant negative PPAR $\beta$  isoform completely abolished the stimulatory effect of GW0742 on CnA $\beta$  promoter activity (Figure 5C). Transient co-transfection with a PPAR $\beta$  expression construct enhanced CnA $\beta$  promoter activity more than six-fold (Figure 5D). A sequence region containing a predicted PPAR-responsive element (PPRE) with 70% identity to the FAT-PPRE<sup>27</sup> was identified in the CnA $\beta$  promoter. Using chromatin immunoprecipitation, we show that PPAR $\beta$  protein associates with this region, whereas no interaction could be detected in the 3'UTR of CnA. An antibody against acetylated histone H3 was used to check for nucleosome integrity (Figure 5E). Electrophoretic mobility shift assays confirmed binding of PPAR $\beta$  to a 26 bp oligonucleotide from the CnA $\beta$  promoter. Incubation with different PPAR $\beta$  antibodies supershifted the retardation bands. The published PPAR $\beta$  binding oligonucleotide from the acyl-CoA oxidase gene (Aco)<sup>28</sup> served as positive control (Figure 5F). Deletion of the identified binding site from the CnA $\beta$  promoter construct completely abolished activation by co-transfection of the PPAR $\beta$  expression construct (Figure 5G).

*The calcineurin inhibitor cyclosporine A abolishes PPAR $\beta$ - induced cardiac growth and vascularization*

Finally, to investigate the *in vivo* relevance of the PPAR $\beta$ - calcineurin interaction for cardiac growth and angiogenesis, we blocked the calcineurin activity in mice under pharmacological PPAR $\beta$  stimulation by parallel injection of cyclosporine A (CsA). Blocking calcineurin activity reduced the relative heart to body weight to control values, blocked the increase in cardiac cell diameters in response to GW0742 injection, and normalized the cell size distribution (Figure 6A). Furthermore, NFATc3 nuclear translocation was blocked by

cyclosporine A (Figure 6B), and the angiogenic response to PPAR $\beta$  stimulation inhibited as indicated by the lower number of isolectin B4-positive vessels (Figure 6C).

## Discussion

The major findings of the present study are the rapid induction of cardiac growth and angiogenesis in response to pharmacological PPAR $\beta$  activation, which are mediated via direct transcriptional stimulation of calcineurin. The growth-promoting effect seems to be restricted to the heart, as we did not observe any alterations in liver or kidney. Recently, we reported a fibre remodelling in skeletal muscle in response to PPAR $\beta$  stimulation, which resulted in an increase in the number of oxidative myofibres and hyperplasia<sup>11</sup>. Interestingly, this hyperplasia in tibialis anterior muscle was accompanied by a reduced size of the myofibres, which is the opposite effect evoked in cardiac muscle cells. The morphological enlargement of cardiomyocytes was accompanied by increased expression of molecular markers of cardiac growth, i.e.  $\alpha$ - and  $\beta$ - myosin heavy chains, calcineurin, and ANF, whereas angiotensinogen was unchanged. Whether the cardiomyocyte enlargement corresponds to pathological or physiological hypertrophy, was not possible to judge from the increase in the above mentioned markers as the calcineurin-NFAT pathway has been described to be important for normal cardiac growth<sup>29, 30</sup> and pathological hypertrophy (reviewed in 31). Also ANF is not only elevated in pathological hypertrophy, but upregulated in physiological cardiac growth in response to moderate non-exhausting exercise<sup>32</sup>. Importantly, echocardiographic examination revealed no functional abnormalities in response to PPAR $\beta$  activation. Morphological and ultra-structural comparison with hearts from mice undergoing long-term voluntary exercise training showed a high degree of similarity to the effects of short-term PPAR $\beta$  activation. On the ultra-structural level, PPAR $\beta$  stimulation resembled physical exercise, i.e. addition of sarcomeres, dense mitochondrial cristae, no signs of cardiomyocyte damage or fibrosis were observed. The slight decrease in collagen content after long-term training or PPAR $\beta$  stimulation is in agreement with inhibition of collagen expression in response to PPAR $\beta$  activation<sup>33</sup>. TUNEL labelling as a marker for DNA damage or repair was not evident after

PPAR $\beta$  stimulation or long-term moderate exercise. This corresponds to a previous report showing prevention of stress-induced apoptosis in cardiomyoblasts upon PPAR $\beta$  activation<sup>34</sup>. The notion of a “physiological” hypertrophy in response to PPAR $\beta$  stimulation is supported by recent data providing evidence that agonists for PPAR $\beta$  and AMP activated protein kinase (AMPK) have exercise mimetic effects in skeletal muscle<sup>35</sup>. In this study, long-term pharmacological PPAR $\beta$  activation in combination with exercise training increased running time of mice by 68% and running distance by 70% over vehicle-treated trained mice. Unfortunately, potential effects on cardiac performance or morphology were not investigated. Based on our data it is tempting to speculate that these modifications occur much more rapidly than within the five weeks interval tested in this study.

As “physiological” hypertrophy is accompanied by increased vascularization whereas pathological hypertrophy is, on the contrary, characterized by a relative lack of capillaries<sup>36</sup>, we analysed a potential cardiac angiogenic response to PPAR $\beta$  stimulation. In agreement with the reported endothelial cell proliferation and angiogenesis *in vitro*<sup>37</sup>, we observed an increased capillary density in the hearts after GW0742 and GW501516 injection. The angiogenic response to PPAR $\beta$  stimulation preceded cardiomyocyte growth, but does not seem to be necessary for cardiomyocyte enlargement, as also in adult cardiomyocytes *in vitro*, PPAR $\beta$  stimulation induced hypertrophy. The fast angiogenic response might contribute to the protection against ischemia/reperfusion injury detected in PPAR $\beta$  transgenic mice<sup>15</sup> and, to our knowledge, represents the most rapid pharmacological approach to induce cardiac vascularization. Whether the PPAR $\beta$ -induced angiogenesis is sufficient to protect against ischemia/reperfusion injury and might improve cardiac function after myocardial infarction is subject of further studies. However, the reversibility of cardiac growth and vascularization 4 weeks after the end of GW0742 treatment points to a potential pharmacological use.

The cardiac growth promoting and pro-angiogenic effects seem to be specific for PPAR $\beta$ , as GW0742 and GW501516 had similar effects whereas the PPAR $\alpha$  agonist clofibrate did not evoke alterations in a similar time-frame. Furthermore, the notion of physiological cardiac growth in response to specific PPAR $\beta$  activation is in agreement with a recent report showing that cardiac-specific PPAR $\beta$  knockout mice develop cardiomyopathy<sup>38</sup>.

As the most likely molecular mechanism for GW0742- and GW501516-induced cardiac growth and angiogenesis, we identified the calcineurin-NFAT pathway. Several lines of evidence suggest that calcineurin represents a direct relevant target of PPAR $\beta$  in cardiac growth and angiogenesis. PPAR $\beta$  activation resulted in up-regulation of calcineurin on the RNA and protein level. Both proteins are co-expressed in adult mouse hearts *in vivo* and in neonatal cardiomyocyte cultures. Furthermore, the calcineurin target genes NFATc3, Hif-1 $\alpha$ , and Cdk9 were stimulated in response to PPAR $\beta$  activation. We can't exclude the possibility that the rapid induction of calcineurin and Hif-1 in response to PPAR $\beta$  stimulation in adult animals *in vivo* involves mRNA or protein stabilisation, but the results obtained in neonatal cardiomyocytes *in vitro* do not support this hypothesis. The activation of the calcineurin promoter in response to pharmacological PPAR $\beta$  stimulation and co-transfection with a PPAR $\beta$  expression construct suggests transcriptional regulation. The effect of GW0742 on calcineurin promoter activity is specific for PPAR $\beta$  as co-transduction with a dominant negative PPAR $\beta$  isoform abolished activation of the promoter construct. In addition, in chromatin immunoprecipitation experiments, we could detect binding of PPAR $\beta$  protein to a promoter sequence, but not to the 3'-UTR of calcineurin. This promoter sequence contained a PPAR responsive element with high homology to the published FAT-binding site<sup>27</sup>. In electrophoretic mobility shift assays, we observed binding of PPAR $\beta$  protein to this predicted PPAR responsive element. Deletion of the PPAR responsive element from the calcineurin

promoter abolished activation by PPAR $\beta$  in transient co-transfection experiments. Finally, although we cannot exclude that cyclosporine A might, beside calcineurin, target other signalling pathways, inhibition of the cardiac growth promoting and pro-angiogenic responses to PPAR $\beta$  activation *in vivo* by CsA underlines the importance of the calcineurin-NFAT pathway for the observed phenotype.

Taken together, we provide evidence that pharmacological PPAR $\beta$  stimulation rapidly induces cardiac angiogenesis and cardiomyocyte growth, which is at least in part mediated via direct transactivation of calcineurin. Echocardiographic examination revealed no functional abnormalities in response to PPAR $\beta$  activation. The short-term PPAR $\beta$  stimulation was able to mimic in the heart the beneficial effects of long-term voluntary physical exercise. Finally, as PPAR $\beta$  activation is known to reduce the size of experimental myocardial infarctions, which is most likely due to our observed rapid induction of angiogenesis, it could have therapeutic potential in treating chronic ischemic heart disease and myocardial infarction.

**Funding**

The work was supported by grants to KDW from Fondation Recherche Medicale, Fondation Cœur et Artères, and Association pour la Recherche sur le Cancer, to PG from Agence National de la Recherche (ANR-05-PCOD-012) and Fondation Cœur et Artères. NW was the recipient of a fellowship from the Fondation de France.

**Acknowledgments**

GW0742 was a generous gift from T.M. Willson (GlaxoSmithKline). The CnA $\beta$  promoter was kindly provided by J. Molkentin. The CREB antibody was a gift of M. Montminy. We thank M. Aupetit, M. Radjkhumar, F. Millot, J. Paput, G. Manfroni, and G. Visciano for technical assistance.

**Conflict of Interest:** none declared.

## References

1. Sher T, Yi HF, McBride OW, Gonzalez FJ. cDNA cloning, chromosomal mapping, and functional characterization of the human peroxisome proliferator activated receptor. *Biochemistry* 1993;**32**:5598-5604.
2. Keech A, Simes RJ, Barter P, Best J, Scott R, Taskinen MR *et al.* FIELD study investigators. Effects of long-term fenofibrate therapy on cardiovascular events in 9795 people with type 2 diabetes mellitus (the FIELD study): randomised controlled trial. *Lancet* 2005;**366**:1849-1861.
3. Dormandy JA, Charbonnel B, Eckland DJ, Erdmann E, Massi-Benedetti M, Moules IK *et al.* PROactive investigators. Secondary prevention of macrovascular events in patients with type 2 diabetes in the PROactive Study (PROspective pioglitAzone Clinical Trial In macroVascular Events): a randomised controlled trial. *Lancet* 2005;**366**:1279-1289.
4. Grimaldi PA. Regulatory functions of PPARbeta in metabolism: implications for the treatment of metabolic syndrome. *Biochim Biophys Acta* 2007;**1771**:983-990.
5. Kliewer SA, Umesono K, Noonan DJ, Heyman RA, Evans RM. Convergence of 9-cis retinoic acid and peroxisome proliferator signalling pathways through heterodimer formation of their receptors. *Nature* 1992;**358**:771-774.
6. Michalik L, Auwerx J, Berger JP, Chatterjee VK, Glass CK, Gonzalez FJ *et al.* International Union of Pharmacology. LXI. Peroxisome proliferator-activated receptors. *Pharmacol Rev* 2006;**58**:726-741.
7. Leibowitz MD, Fiévet C, Hennuyer N, Peinado-Onsurbe J, Duez H, Bergera J *et al.* Activation of PPARdelta alters lipid metabolism in db/db mice. *FEBS Lett* 2000;**473**:333-336.
8. Tanaka T, Yamamoto J, Iwasaki S, Asaba H, Hamura H, Ikeda Y *et al.* Activation of peroxisome proliferator-activated receptor delta induces fatty acid beta-oxidation in

- skeletal muscle and attenuates metabolic syndrome. *Proc Natl Acad Sci U S A* 2003;**100**:15924-15929.
9. Holst D, Luquet S, Nogueira V, Kristiansen K, Leverve X, Grimaldi PA. Nutritional regulation and role of peroxisome proliferator-activated receptor delta in fatty acid catabolism in skeletal muscle. *Biochim Biophys Acta* 2003;**1633**:43-50.
  10. Luquet S, Lopez-Soriano J, Holst D, Fredenrich A, Melki J, Rassoulzadegan, M *et al.* Peroxisome proliferator-activated receptor delta controls muscle development and oxidative capability. *FASEB J* 2003;**17**:2299-2301.
  11. Gaudel, C, Schwartz C, Giordano C, Abumrad NA, Grimaldi PA. Pharmacological activation of PPAR{beta} promotes rapid and calcineurin-dependent fiber remodeling and angiogenesis in mouse skeletal muscle. *Am J Physiol Endocrinol Metab* 2008;**295**:E297-E304.
  12. Wang YX, Zhang CL, Yu RT, Cho HK, Nelson MC, Bayuga-Ocampo *et al.* Regulation of muscle fiber type and running endurance by PPARdelta. *PLoS Biol* 2004;**2**:e294.
  13. Cheng L, Ding G, Qin Q, Xiao Y, Woods D, Chen YE *et al.* Peroxisome proliferator-activated receptor delta activates fatty acid oxidation in cultured neonatal and adult cardiomyocytes. *Biochem Biophys Res Commun* 2004;**313**:277-286.
  14. Kim HJ, Ham SA, Kim SU, Hwang JY, Kim JH, Chang KC *et al.* Transforming growth factor-beta1 is a molecular target for the peroxisome proliferator-activated receptor delta. *Circ Res* 2008;**102**:193-200.
  15. Burkart EM, Sambandam N, Han X, Gross RW, Courtois M, Gierasch CM *et al.* Nuclear receptors PPARbeta/delta and PPARalpha direct distinct metabolic regulatory programs in the mouse heart. *J Clin Invest* 2007;**117**:3930-3939.

16. Wagner KD, Wagner N, Ghanbarian H, Grandjean V, Gounon P, Cuzin F *et al.* RNA induction and inheritance of epigenetic cardiac hypertrophy in the mouse. *Dev Cell* 2008;**14**:962-969.
17. Buchwalow IB, Schulze W, Kostic MM, Wallukat G, Morwinski R. Intracellular localization of inducible nitric oxide synthase in neonatal rat cardiomyocytes in culture. *Acta Histochem* 1997;**99**:231-240.
18. Oka T, Dai YS, Molkentin JD. Regulation of calcineurin through transcriptional induction of the calcineurin A beta promoter in vitro and in vivo. *Mol Cell Biol* 2005;**25**:6649-6659.
19. Bastie C, Luquet S, Holst D, Jehl-Pietri C, Grimaldi PA. Alterations of peroxisome proliferator-activated receptor delta activity affect fatty acid-controlled adipose differentiation. *J Biol Chem* 2000;**275**:38768-38773.
20. Wagner N, Wagner KD, Theres H, Englert C, Schedl A, Scholz H. Coronary vessel development requires activation of the TrkB neurotrophin receptor by the Wilms' tumor transcription factor Wt1. *Genes Dev* 2005;**19**:2631-2642.
21. Koda M, Takemura G, Kanoh M, Hayakawa K, Kawase Y, Maruyama R *et al.* Myocytes positive for in situ markers for DNA breaks in human hearts which are hypertrophic, but neither failed nor dilated: a manifestation of cardiac hypertrophy rather than failure. *J Pathol* 2003;**199**:229-236.
22. Shohet RV, Garcia JA. Keeping the engine primed: HIF factors as key regulators of cardiac metabolism and angiogenesis during ischemia. *J Mol Med* 2007;**85**:1309-1315.
23. Michele DE, Gomez CA, Hong KE, Westfall MV, Metzger JM. Cardiac dysfunction in hypertrophic cardiomyopathy mutant tropomyosin mice is transgene-dependent, hypertrophy-independent, and improved by beta-blockade. *Circ Res* 2002;**91**:255-62.

24. Wilkins BJ, Molkenin JD. Calcium-calcineurin signaling in the regulation of cardiac hypertrophy. *Biochem Biophys Res Commun* 2004;**322**:1178-1191.
25. Liu YV, Hubbi ME, Pan F, McDonald KR, Mansharamani M, Cole RN *et al.* 2007. Calcineurin promotes hypoxia-inducible factor 1alpha expression by dephosphorylating RACK1 and blocking RACK1 dimerization. *J Biol Chem* 2007;**282**:37064-37073.
26. Sano M, Abdellatif M, Oh H, Xie M, Bagella L, Giordano A *et al.* Activation and function of cyclin T-Cdk9 (positive transcription elongation factor-b) in cardiac muscle-cell hypertrophy. *Nat Med* 2002;**8**:1310-1317.
27. Frohnert BI, Hui TY, Bernlohr DA. Identification of a functional peroxisome proliferator-responsive element in the murine fatty acid transport protein gene. *J Biol Chem* 1999;**274**:3970-7.
28. Amri EZ, Bonino F, Ailhaud G, Abumrad NA, Grimaldi PA. Cloning of a protein that mediates transcriptional effects of fatty acids in preadipocytes. Homology to peroxisome proliferator-activated receptors. *J Biol Chem* 1995;**270**:2367-71.
29. Yang XY, Yang TT, Schubert W, Factor SM, Chow CW. Dosage-dependent transcriptional regulation by the calcineurin/NFAT signaling in developing myocardium transition. *Dev Biol* 2007;**303**:825-837.
30. Bueno OF, Brandt EB, Rothenberg ME, Molkenin JD. Defective T cell development and function in calcineurin A beta -deficient mice. *Proc Natl Acad Sci U S A* 2002;**99**:9398-9403.
31. Heineke J, Molkenin JD. Regulation of cardiac hypertrophy by intracellular signalling pathways. *Nat Rev Mol Cell Biol* 2006;**7**:589-600.
32. Pan SS. Alterations of atrial natriuretic peptide in cardiomyocytes and plasma of rats after different intensity exercise. *Scand J Med Sci Sports* 2008;**18**:346-353.

33. Zhang H, Pi R, Li R, Wang P, Tang F, Zhou S *et al.* PPARbeta/delta activation inhibits angiotensin II-induced collagen type I expression in rat cardiac fibroblasts. *Arch Biochem Biophys* 2007;**460**:25-32.
34. Pesant M, Sueur S, Dutartre P, Tallandier M, Grimaldi PA, Rochette L *et al.* Peroxisome proliferator-activated receptor delta (PPARdelta) activation protects H9c2 cardiomyoblasts from oxidative stress-induced apoptosis. *Cardiovasc Res* 2006;**69**:440-449.
35. Narkar VA, Downes M, Yu RT, Embler E, Wang YX, Banayo E *et al.* AMPK and PPARdelta agonists are exercise mimetics. *Cell* 2008;**134**:405-415.
36. Leosco D, Rengo G, Iaccarino G, Golino L, Marchese M, Fortunato F *et al.* Exercise promotes angiogenesis and improves beta-adrenergic receptor signalling in the post-ischaemic failing rat heart. *Cardiovasc Res* 2008;**78**:385-94.
37. Piqueras L, Reynolds AR, Hodivala-Dilke KM, Alfranca A, Redondo JM, Hatae T *et al.* Activation of PPARbeta/delta induces endothelial cell proliferation and angiogenesis. *Arterioscler Thromb Vasc Biol* 2007;**27**:63-9.
38. Cheng L, Ding G, Qin Q, Huang Y, Lewis W, He N *et al.* Cardiomyocyte-restricted peroxisome proliferator-activated receptor-delta deletion perturbs myocardial fatty acid oxidation and leads to cardiomyopathy. *Nat Med* 2004;**10**:1245-50.

## Figure Legends

**Figure 1: PPAR $\beta$  activation stimulates cardiac growth.** (A) Hypertrophic development of the ventricular walls 24 hours after GW0742 injection (b) compared to a vehicle-injected control (a). (B) Mean values  $\pm$  S.E.M. of heart to body weight ratios. (C) Mean values  $\pm$  S.E.M. of body weights of control mice and animals injected for different time points with GW0742 ( $n=4$  each). (D) High magnifications of heart sections. (E) Mean values  $\pm$  S.E.M of cardiomyocyte diameters. \*\*\* indicates  $p<0.001$ . (F) Distribution of cardiomyocyte diameters. Note the progressive shift of cell sizes to larger diameters with increasing time of PPAR $\beta$  stimulation. (G) Echocardiographic examination of control mice and animals injected with GW0742 ( $n=7$  each) confirmed the increased septum thickness (a), but revealed no functional disadvantage as indicated by the normal aortic outflow (b), unchanged shortening fraction (c), and preserved left ventricular end-diastolic diameters (LVEDD, d). (F) Hematoxylin-eosin staining of kidney and liver sections of control mice and animals after 24 hours of GW0742 injection shows no obvious abnormalities in these organs. Scale bars: 50  $\mu\text{m}$ .

**Figure 2: PPAR $\beta$  induced cardiac growth is reversible and resembles exercise-induced cardiac hypertrophy.** (A) Mean values  $\pm$  S.E.M. of heart to body weight ratios of control mice, animals injected for different time points with GW0742, and mice performing 5 weeks of voluntary exercise ( $n=4$  each). Note that the heart to body weight ratio was still increased 10 days after the end of the treatment, but returned to control values 4 weeks after the end of the treatment. The degree of cardiac growth due to GW0742 injection was comparable to physiological cardiac hypertrophy induced by 5 weeks of voluntary exercise. \*\* indicates  $p<0.01$  (B) Mean values  $\pm$  S.E.M of cardiomyocyte diameters. \* indicates  $p<0.05$  and \*\*  $p<0.01$ . (C) Distribution of cardiomyocyte diameters from mice after GW0742 injection, voluntary exercise training, and respective controls. (D) Electron microscopic examination of

the hearts after GW0742 injection (b, e) revealed no signs of pathological cardiac hypertrophy compared to controls (a, d), but addition of sarcomeres, dense mitochondrial cristae, and normal sarcomere lengths, which was comparable to cardiac hypertrophy induced by voluntary exercise for 5 weeks (c, f). Scale bars: 5  $\mu\text{m}$  in a, b, c; 2  $\mu\text{m}$  in d, e, f. (E) Sirius Red staining was used to detect collagen fibres (red). (F) Quantification of Sirius Red staining. Note that PPAR $\beta$  activation and exercise training slightly reduced the collagen content. (G) Quantification of the number of TUNEL-positive cells per field as a marker of apoptosis. (H) Representative photomicrographs for TUNEL staining (DAB substrate, brown colour). Note that TUNEL staining revealed no differences between mice after GW0742 injection, voluntary exercise training, and controls. A section from a mouse model with cardiomyopathy<sup>16</sup> served as positive control. Scale bars: 50  $\mu\text{m}$ .

**Figure 3: Pharmacological PPAR $\beta$  stimulation induces rapidly cardiac angiogenesis.**

(A) Expression of Hif-1 $\alpha$ , a known regulator of angiogenesis<sup>22</sup>, was increased 5 and 24 hours after GW0742 injection on an immunohistological level (b, c). (B) Western Blot analysis of Hif-1 $\alpha$  and PECAM-1 (CD31) as a marker of proliferating endothelial cells.  $\alpha$ -tubulin served as an internal standard. (C) Expression of PECAM-1 (CD31) was stimulated after 5 and 24 hours in response to PPAR $\beta$  activation on the immunohistological level (b, c), which was quantified by counting of PECAM-1 positive vessels per field (d). (D) Isolectin B4 staining was used to identify all vascular cells (a-c). Morphometric analysis revealed a higher number of vessels in response to PPAR $\beta$  activation (d). Scale bars: 50  $\mu\text{m}$ . \*\*\* indicates  $p < 0.001$ .

**Figure 4: Markers of cardiac growth and angiogenesis are up-regulated in response to PPAR $\beta$  activation.**

(A) Quantitative RT-PCR analysis of the levels of  $\alpha$ -myosin heavy chain ( $\alpha$ -MHC, Myh6),  $\beta$ -MHC (Myh7), angiotensinogen, atrial natriuretic factor (ANF), and calcineurin in the hearts at different time points after PPAR $\beta$  stimulation. \* $p < 0.05$ , \*\* $p < 0.01$ , \*\*\* $p < 0.001$ . (B) Western Blot analysis of PPAR $\beta$  and calcineurin expression at different

time points after PPAR $\beta$  stimulation. Note the strong increase in calcineurin expression while PPAR $\beta$  remains unchanged.  $\alpha$ -tubulin served as an internal standard. (C) Immunohistochemical localization of NFATc3, which becomes nuclearised already 5 hours after PPAR $\beta$  activation. (D) Subcellular fractionation in cytoplasmic (C), nuclear (N), and insoluble (I) proteins and subsequent Western Blot analysis. Note the increased nuclear expression of NFATc3 and Hif-1 $\alpha$  in response to PPAR $\beta$  activation. CREB (nuclear), Rho GDI $\alpha$  (cytoplasmic), and acetylated histone H3 (H3, chromatin associated) antibodies were used to evaluate the purity of each fraction. (E) Immunohistological and Western Blot analysis of Cdk9 expression in response to PPAR $\beta$  activation. Note the increased Cdk9 expression already after 5 hours. Scale bars: 50  $\mu$ m.

**Figure 5: PPAR $\beta$  directly transcriptionally activates calcineurin.** (A) Immunohistological localisation of PPAR $\beta$  (red) and calcineurin (green) in adult mouse hearts (a, b) *in vivo* and in isolated neonatal cardiomyocytes *in vitro* (c, d). Note the nuclear PPAR $\beta$  and cytoplasmic calcineurin expression in the same cells. Scale bars: 50  $\mu$ m. (B) Transient transfections of the calcineurin A $\beta$  promoter in a luciferase vector in the presence of 100nM GW0742 or vehicle in primary neonatal mouse cardiomyocytes. Luciferase activities were normalized for the activity of co-transfected  $\beta$ -galactosidase ( $n=7$ , \* $p<0.05$ ). (C) Transient transfection of the calcineurin A $\beta$  promoter construct in the presence of 200nM GW0742 or vehicle with additional retroviral transduction of primary neonatal cardiomyocytes with a dominant negative isoform of PPAR $\beta$  (PPAR $\beta$ DN). Note that in the presence of PPAR $\beta$ DN, GW0742 did not activate the calcineurin promoter ensuring specificity of the GW0742 effect for PPAR $\beta$  ( $n=4$ , \* $p<0.05$ ). (D) Transient co-transfection of the calcineurin A $\beta$  promoter construct together with a PPAR $\beta$  expression construct in neonatal cardiomyocytes ( $n=13$ , \* $p<0.05$ ). (E) Chromatin-immunoprecipitation to analyse PPAR $\beta$  protein interaction with

CnA $\beta$ -regulatory sequences. PPAR $\beta$  protein binds to the CnA $\beta$  promoter (upper panel), but not to the 3'-untranslated region (UTR) of CnA $\beta$  (lower panel). Input DNA and immunoprecipitates obtained with acetylated histone 3 antibody served as positive controls. Negative controls were performed with normal serum instead of specific antibodies and with DNase-free water for the PCR. (F) Electrophoretic mobility shift assay demonstrating binding of the PPAR $\beta$ /R $\alpha$  complex to the predicted consensus element of the CnA $\beta$  promoter (arrowhead). Preincubation of the reactions with different PPAR $\beta$  antibodies supershifted the complexes (arrow). Note that the PPAR $\beta$  antibody from rabbit tended to produce negative supershifts as it has been described<sup>28</sup>. An oligonucleotide from the acyl-CoA oxidase gene served as positive control<sup>28</sup>. (G) Transient co-transfection of the wild-type calcineurin A $\beta$  promoter construct or a construct with deletion of the identified 26bp consensus motif together with PPAR $\beta$  expression constructs in neonatal cardiomyocytes ( $n=4$ , \* $p<0.05$ ). Note that the 26bp deletion abolished transactivation by PPAR $\beta$ .

**Figure 6: Blocking the calcineurin activity by cyclosporine A (CsA) inhibits both, PPAR $\beta$ -induced cardiac growth and angiogenesis *in vivo*.** (A) Mean values  $\pm$  S.E.M. of heart to body weight ratios of mice injected with GW0742 or a combination of GW0742 and CsA (a), mean values  $\pm$  S.E.M of cardiomyocyte diameters (b), and distribution of cardiomyocyte diameters (c) \* $p<0.05$ , \*\* $p<0.01$ . (B) Immunohistological localization of NFATc3 in hearts of mice injected with GW0742 (a, b) or a combination of GW0742 and CsA (c, d). Note that CsA inhibits PPAR $\beta$  induced nuclear translocation of NFATc3. (C) Immunohistological detection of Isolectin B4 as a marker for vascular cells. Note that CsA inhibits PPAR $\beta$ - induced angiogenesis in the heart. Scale bars: 50  $\mu$ m.

Figure 1

[Click here to download high resolution image](#)

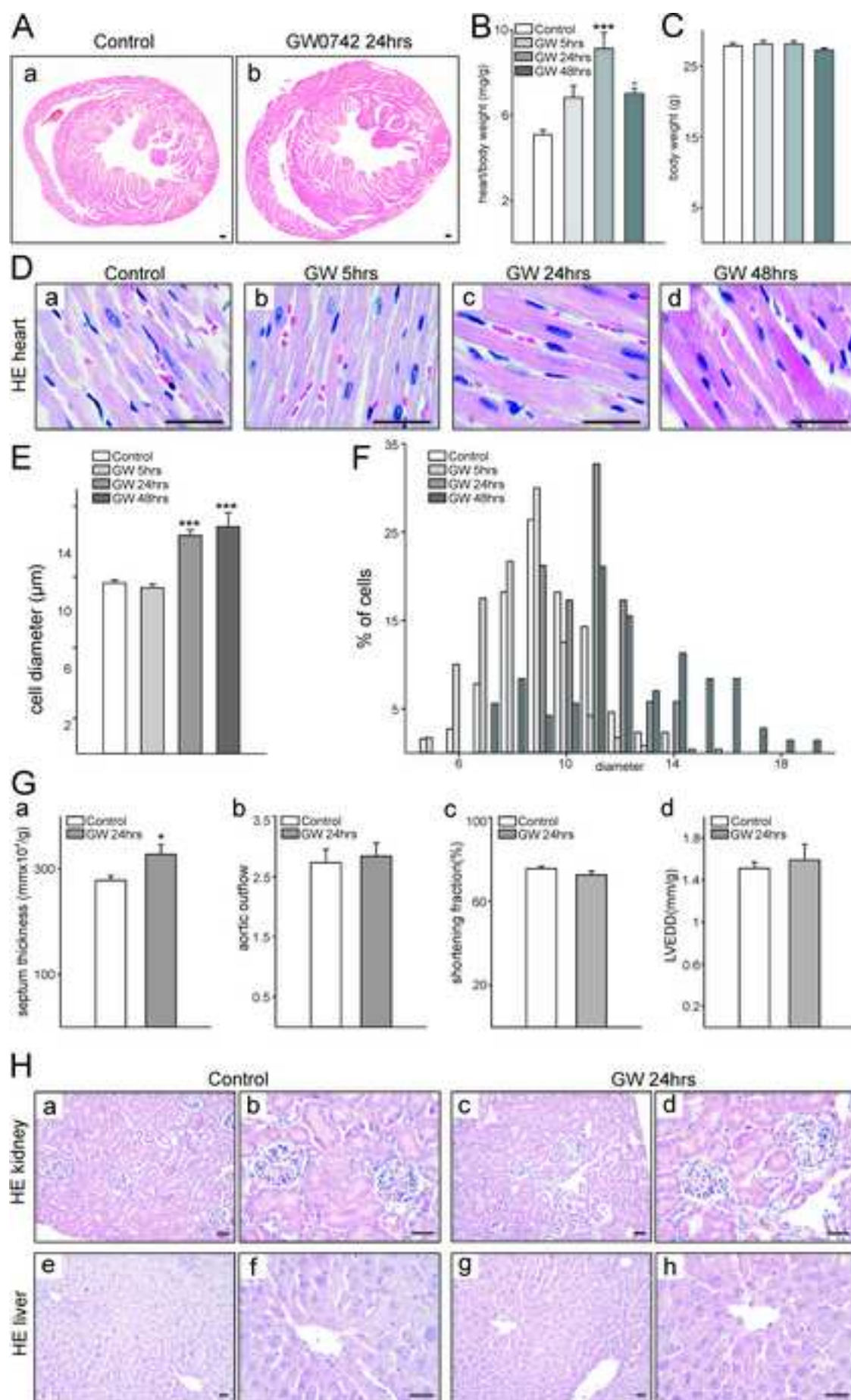
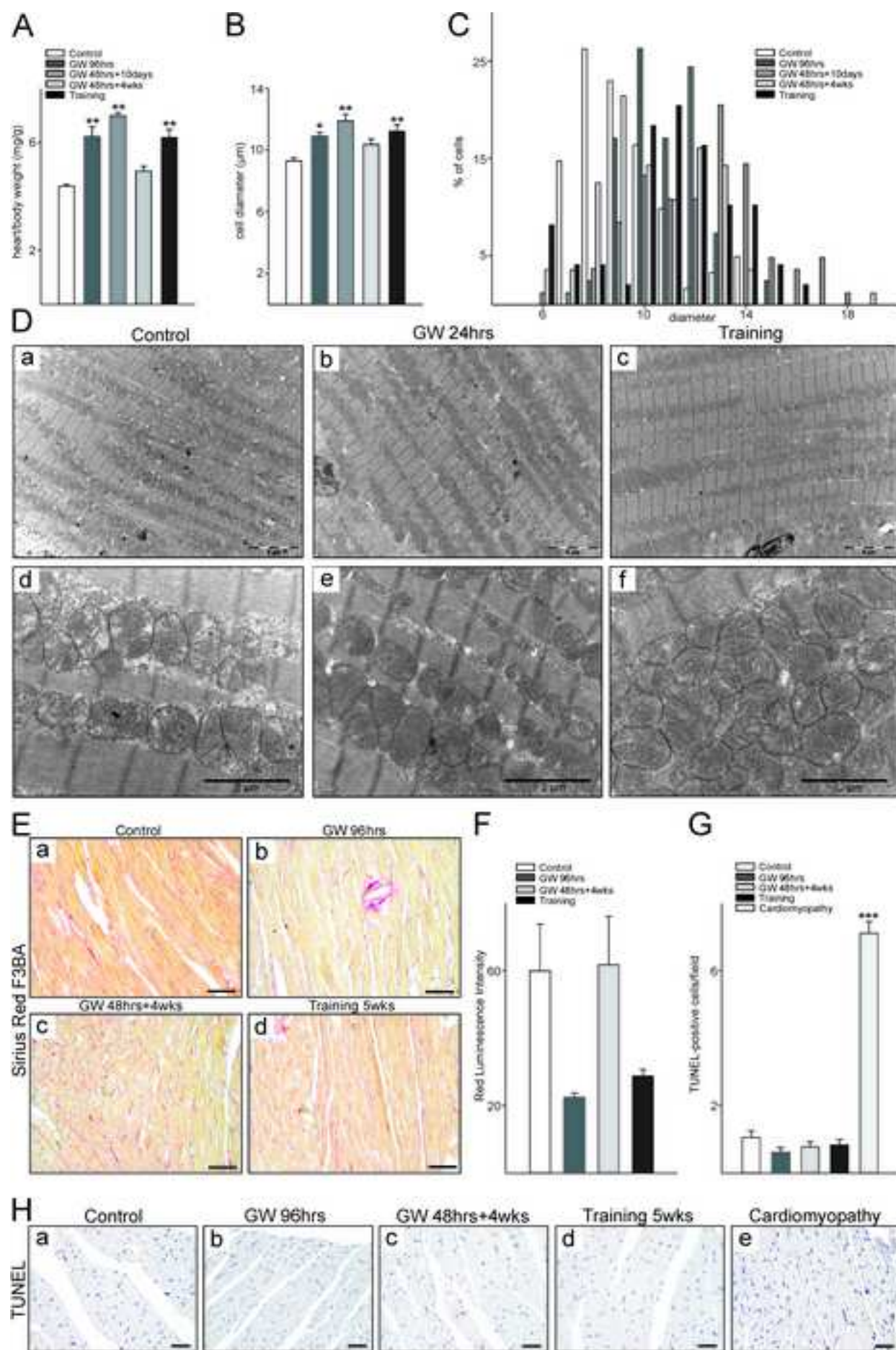


Figure 1

**Figure 2**  
[Click here to download high resolution image](#)



**Figure 2**

Figure3  
[Click here to download high resolution image](#)

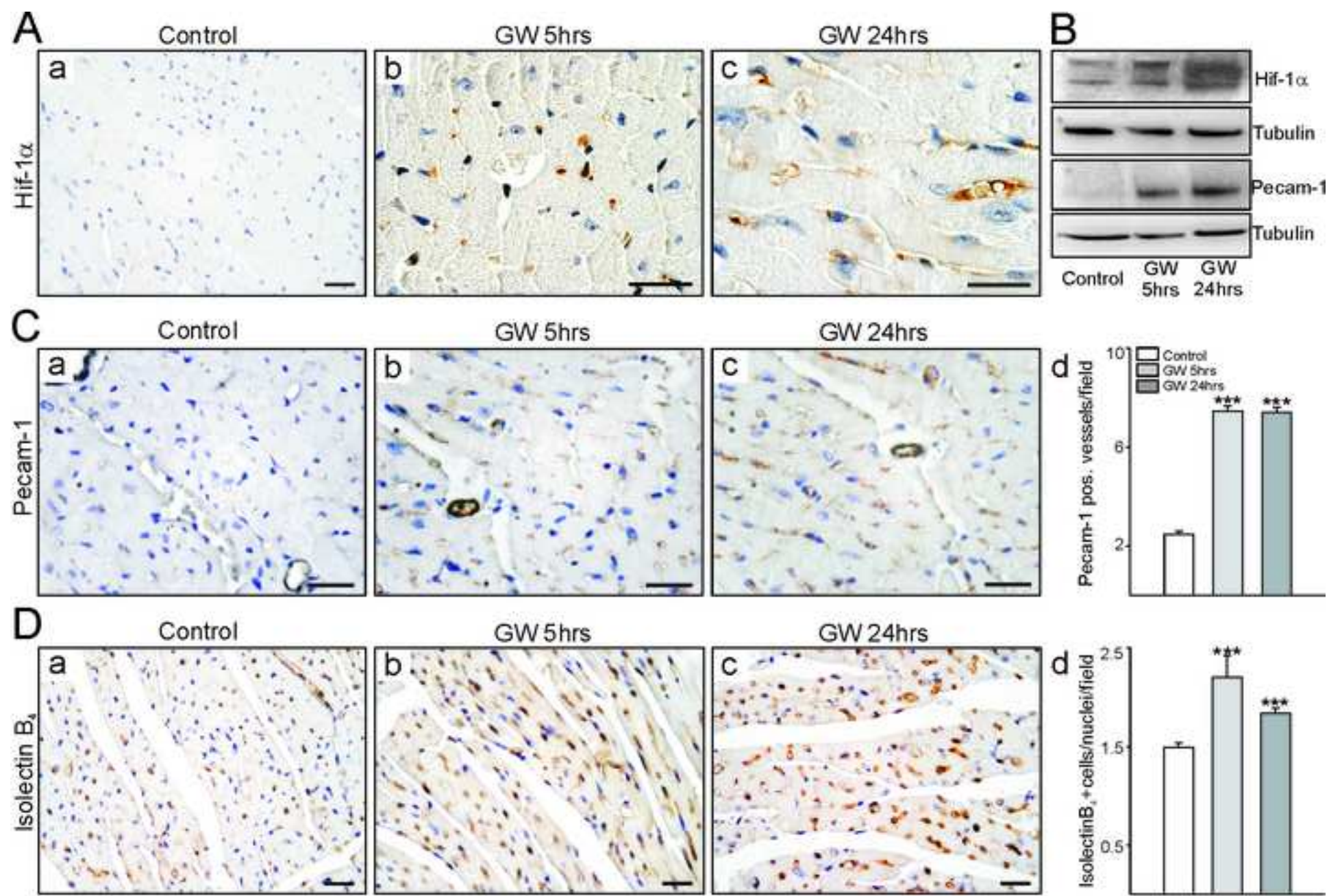
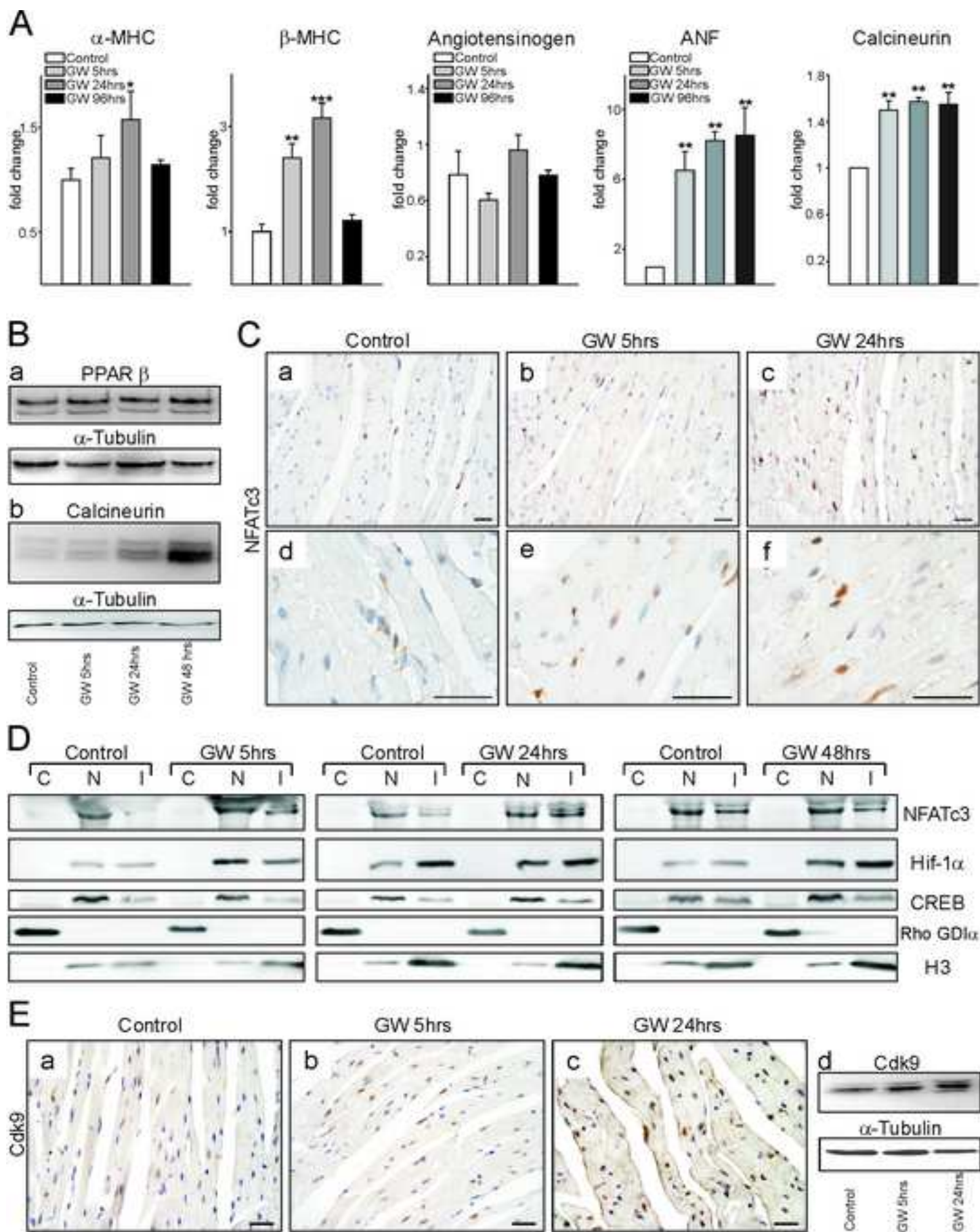


Figure 3

**Figure 4**  
[Click here to download high resolution image](#)



**Figure 4**

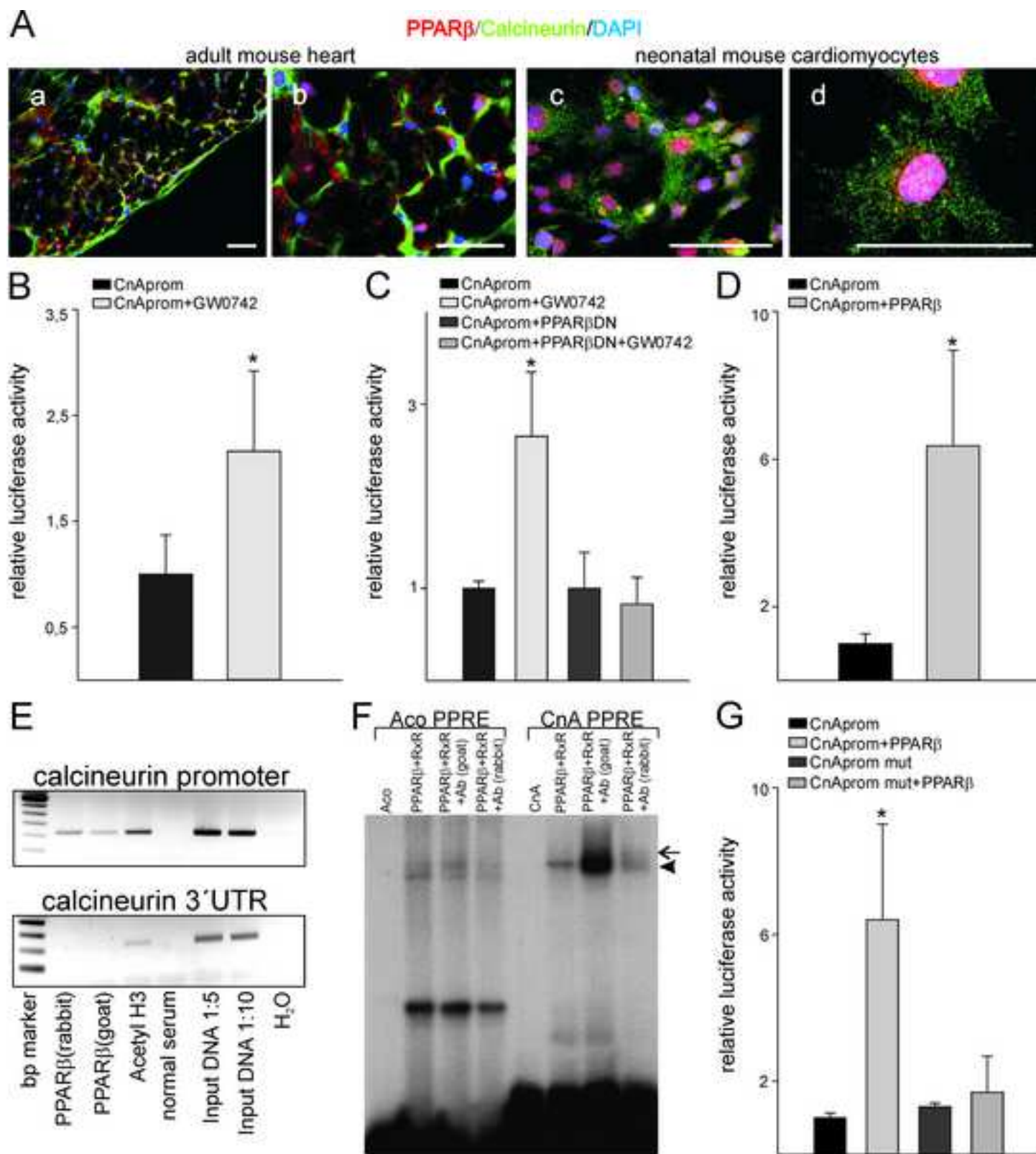
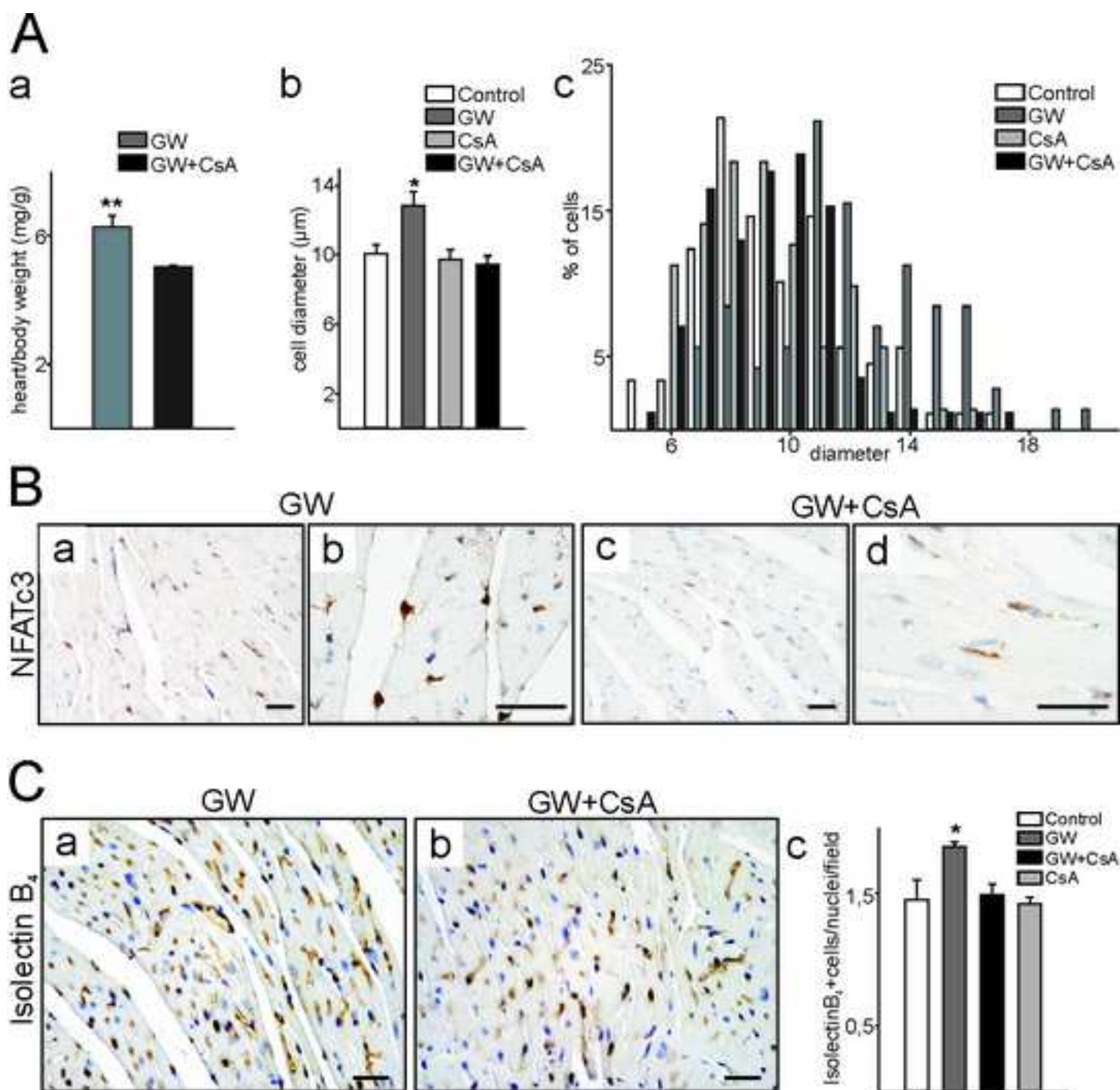
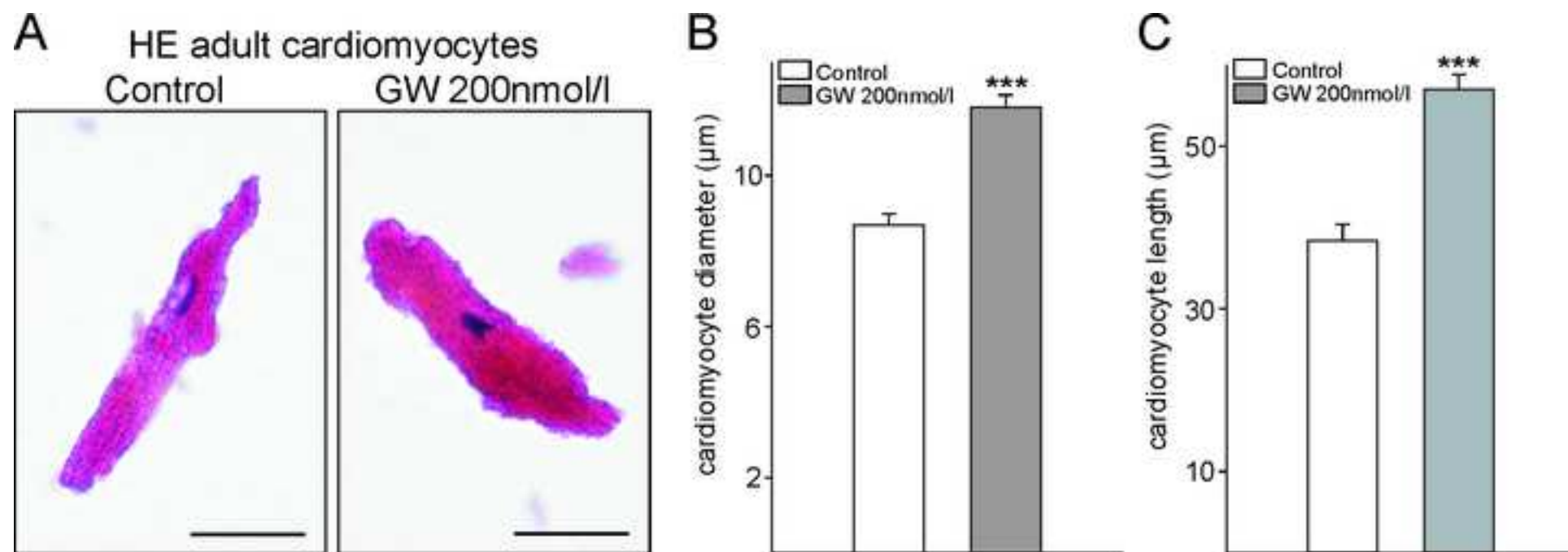


Figure 5

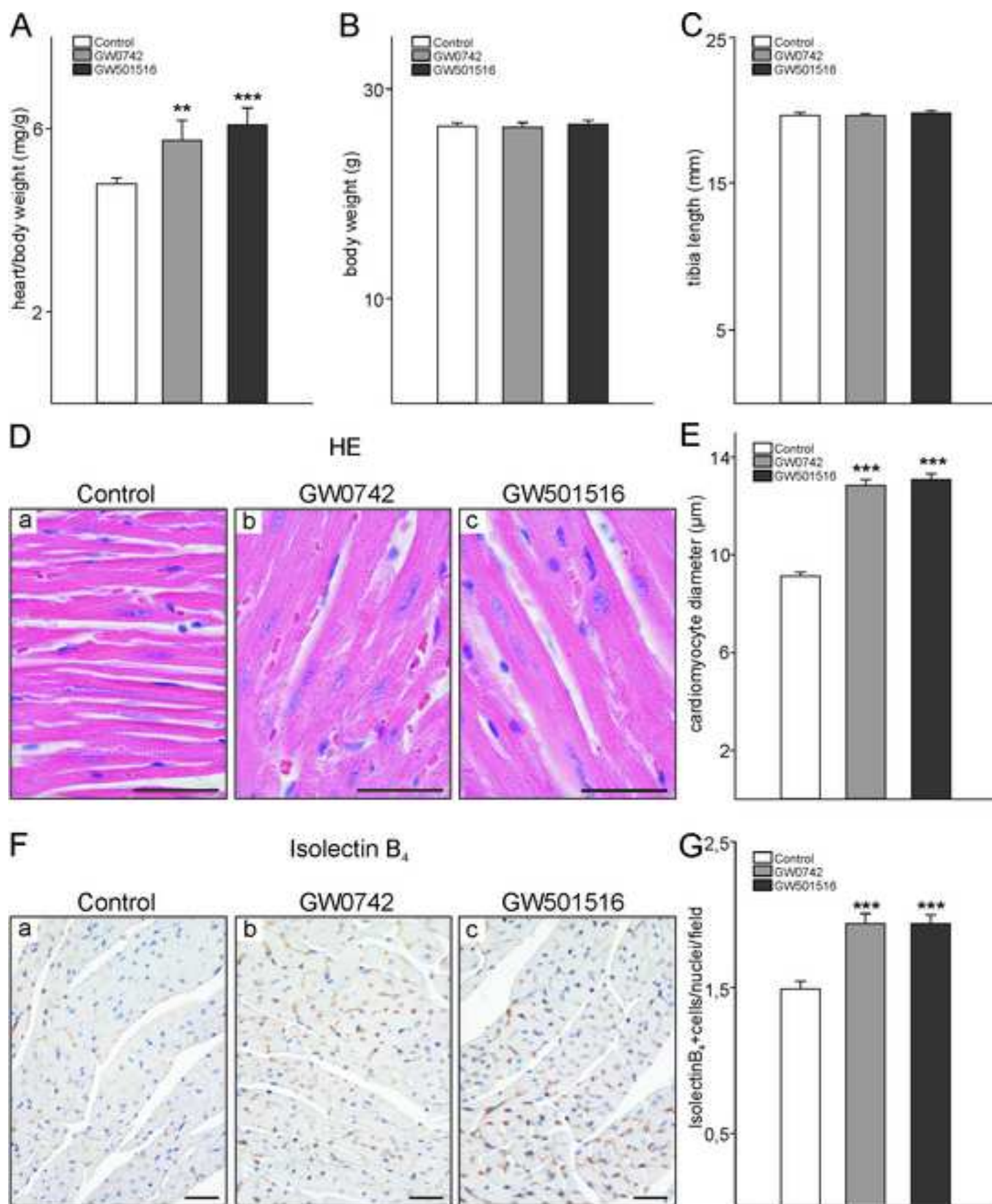
**Figure 6**  
[Click here to download high resolution image](#)



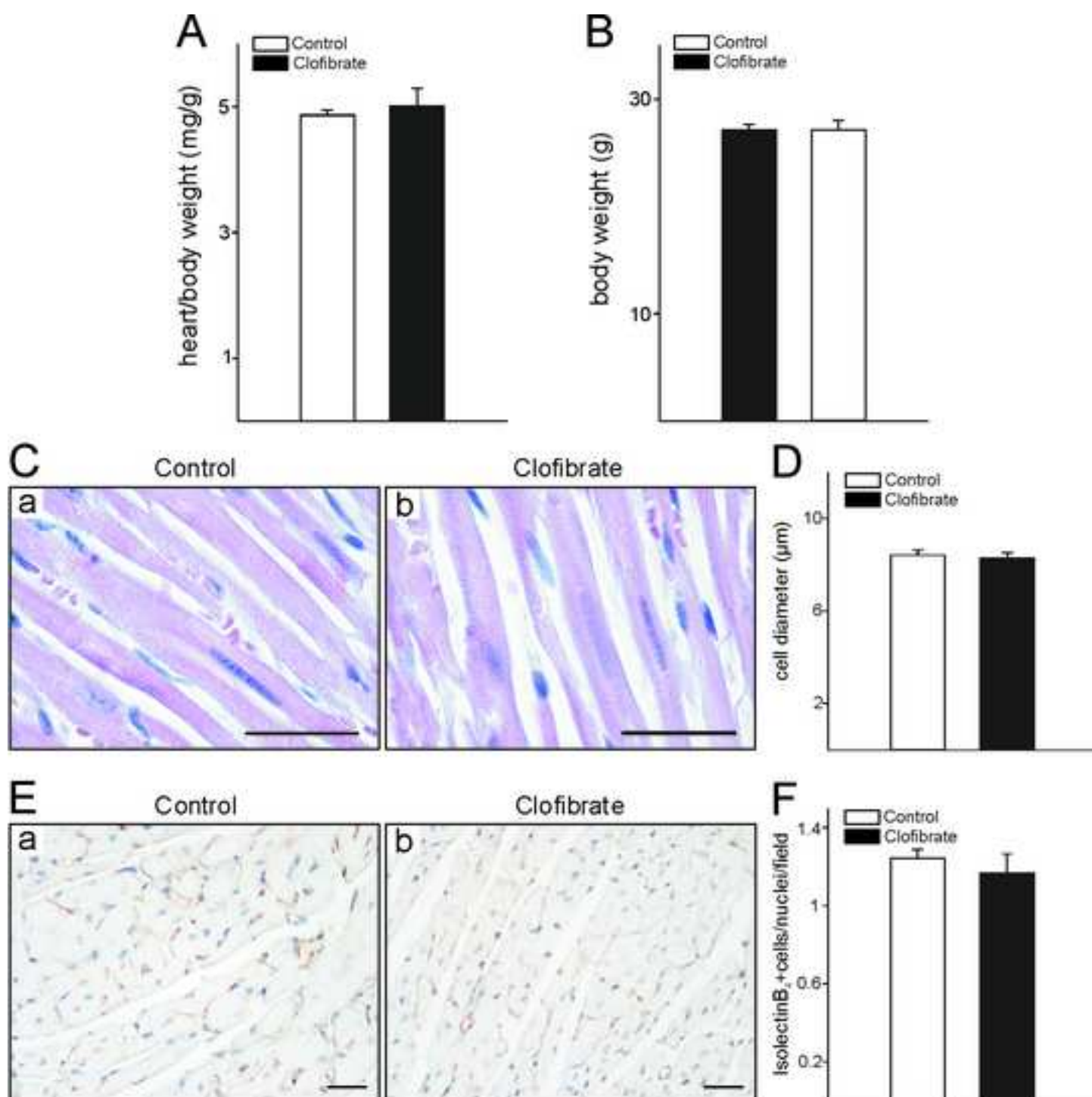
**Figure 6**



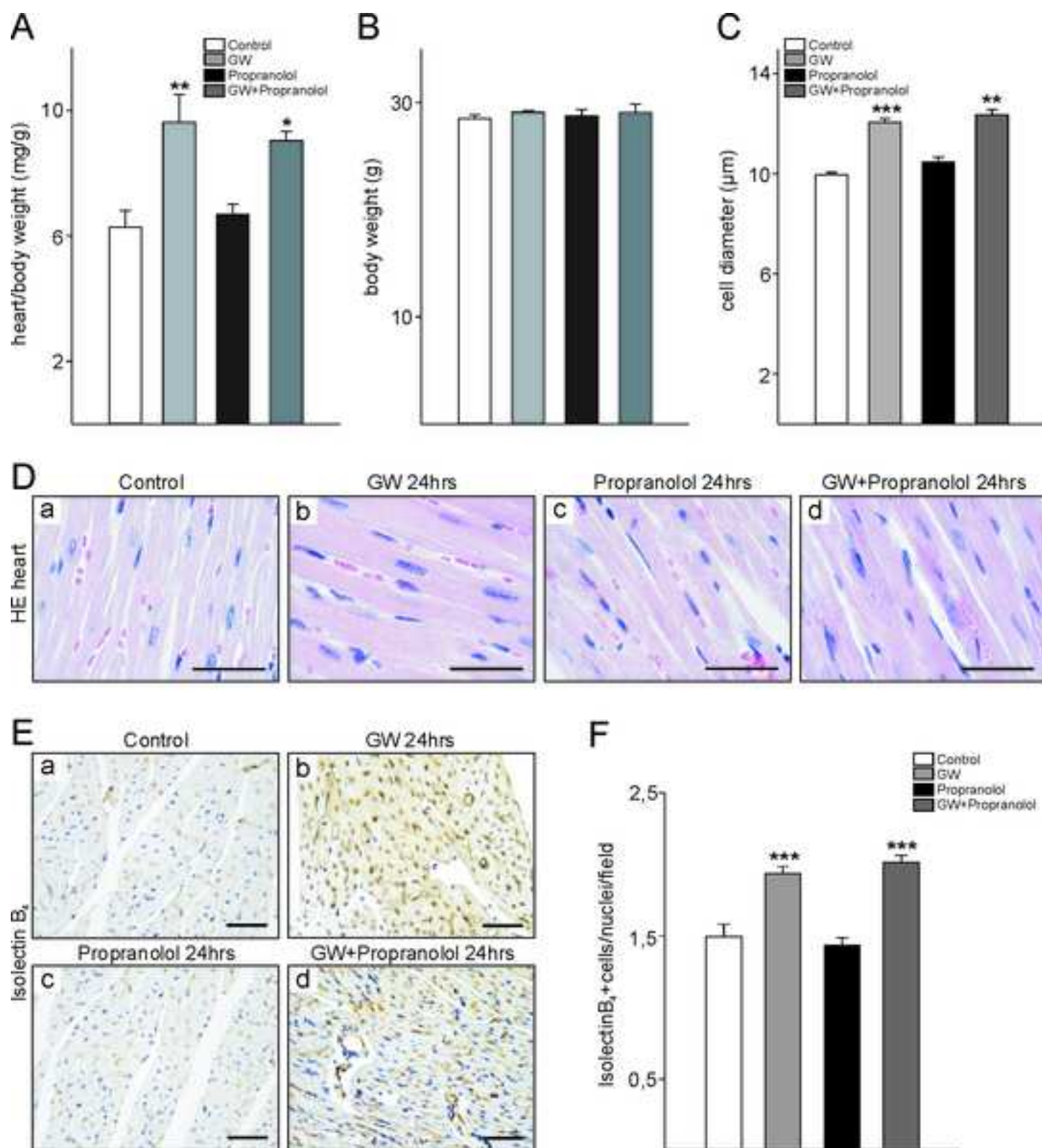
Supplemental Figure 1



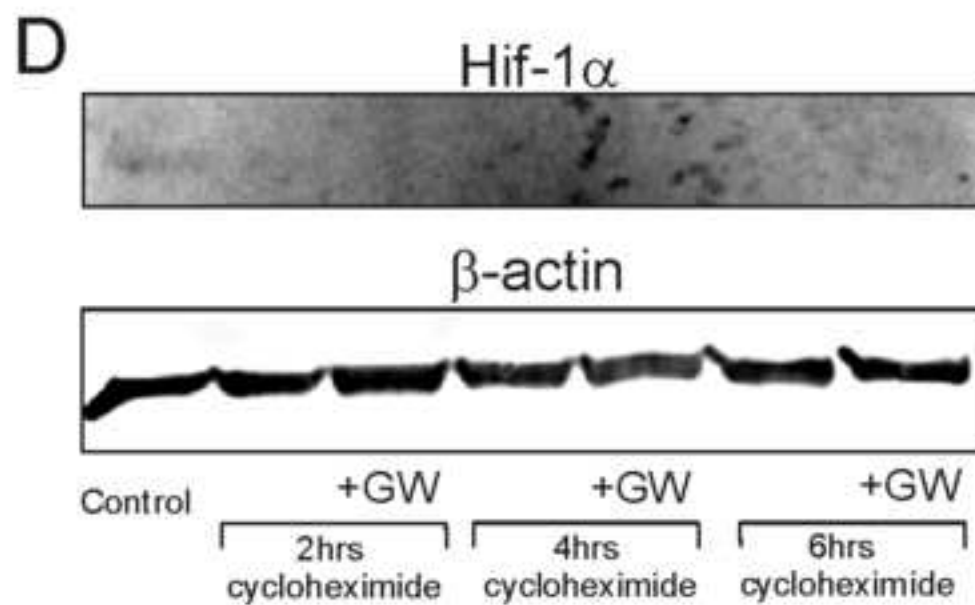
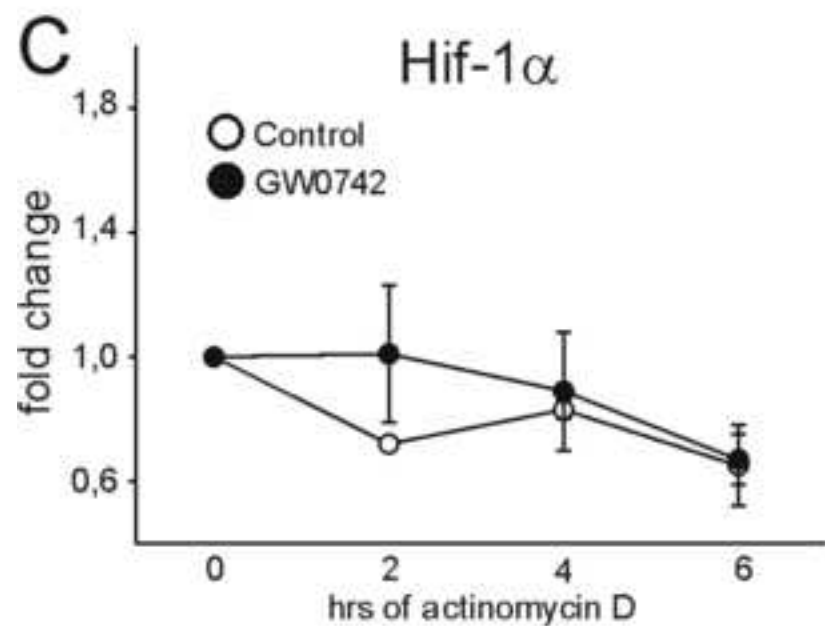
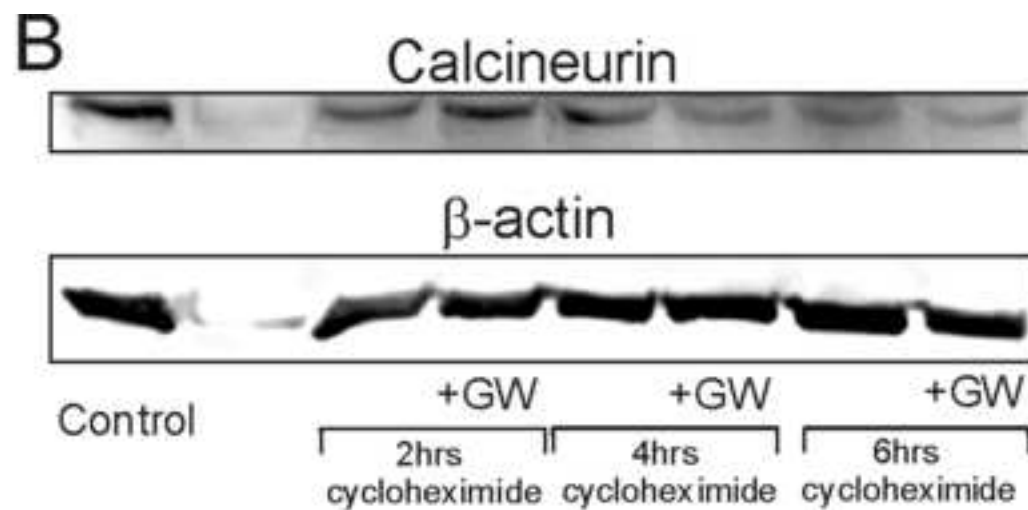
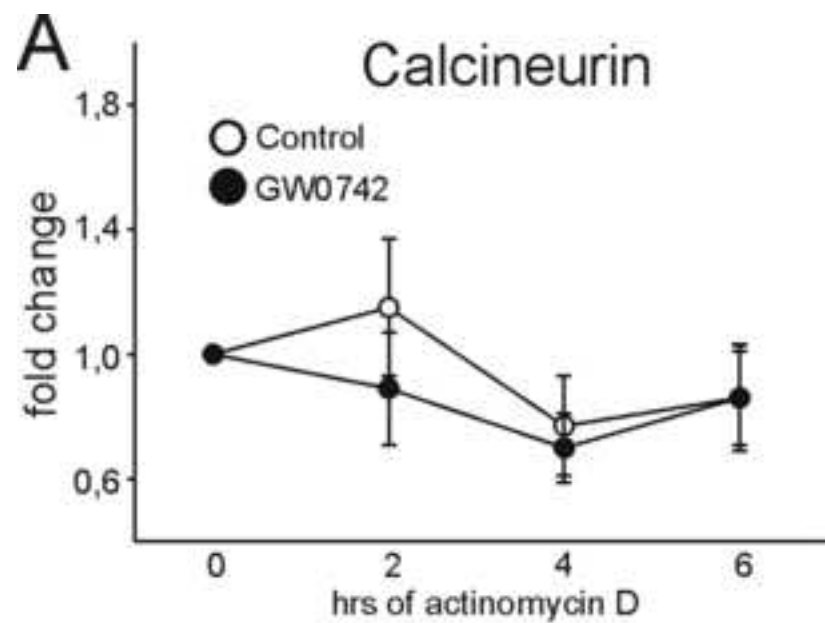
Supplemental Figure 2



Suppl. Figure 3



Supplemental. Figure 4



Supplemental Figure 5

## Methods

### *Animals*

10 weeks old male C57BL6J (Janvier, France) mice were subcutaneously injected with GW0742 (Glaxo Smith Kline) or GW501516 (Alexis Biochemicals) dissolved in DMSO at 1mg/kg once daily (2pm) according to the duration of treatment (24, 48, 96 hrs). Controls received DMSO injections. Cyclosporine A (Sigma) dissolved in DMSO was administered daily (9am) by subcutaneous injection in a dose of 20mg/kg. Clofibrilic acid (Sigma) was injected one time a day (2pm) in a dose of 300mg/kg. Propranolol (Sigma) dissolved in PBS was injected subcutaneously daily in a dose of 0,5mg/kg. Physical training was performed by keeping the animals in cages for voluntary physical exercise (Techniplast, Italy) equipped with a running wheel (25 cm diameter) for five weeks.

### *Histological and immunohistochemical analysis*

Paraffin sections (5µm) were stained with hematoxylin and eosin. Mean cardiomyocyte diameters were determined by a blinded investigator measuring at least 30 cells per heart of four hearts for each condition. Collagen-specific Sirius Red (Waldeck GmbH, Münster, Germany) staining for measurement of interstitial fibrosis was performed according to manufacturer's instructions and quantified in Adobe Photoshop measuring red channel luminescence from sections developed at the same time and photographed with identical camera settings. Antigen detection for Hif-1 $\alpha$ , NFATc3 and CDK9 was performed using the M.O.M. Kit (PK-2200, Vector Laboratories). Mouse monoclonal antibodies CDK9 (D-7, sc-13130, Santa Cruz Biotechnology), HIF 1 $\alpha$  (MAB 5382, Chemicon), and NFATc3 (F-1, sc-8405, Santa Cruz Biotechnology) were used in a 1:100 dilution. Staining for PECAM-1 (M-20, sc-1506, Santa Cruz Biotechnology, 1:100 dilution) was done with a biotinylated anti-goat

antibody (Vector Laboratories), followed by incubation with peroxidase-coupled Streptavidin (Sigma). PECAM-1 positive vessels per field were counted, for each animal 6 fields were investigated, based on a number of four animals per condition and three tissue sections for each animal. Isolectin B4 positive cells were identified using a biotinylated GSL I-isolectin B4 antibody (B-1205, Vector Laboratories) and peroxidase-coupled Streptavidin. DAB (SK-4100, Vector Laboratories) served as a substrate. Nuclei were counterstained with hematoxylin.

For immunofluorescence double labelling, methanol fixed cardiomyocytes or heart cryosections were incubated with a rabbit polyclonal anti-PPAR $\beta$  antibody (H-74, sc-7197, Santa Cruz Biotechnology, 1:100), followed by incubation with a Cy-3 coupled secondary antibody (Jackson ImmunoResearch). Subsequently, calcineurin was detected with a monoclonal mouse antibody (BD Transduction Laboratories, 1:25), using the M.O.M. Kit and FITC-coupled Streptavidin (Sigma). Nuclei were counterstained with DAPI. Slides were viewed under an epifluorescence microscope connected to a digital camera with the Spot software (Universal Imaging Corp.).

#### *TUNEL-labelling of apoptotic cells*

Apoptotic cells were detected by TUNEL staining in paraffin-embedded heart sections using the In situ Cell Death Detection Kit (Roche Molecular Biochemicals) as described previously<sup>16</sup>. TUNEL-positive cells/field were counted. Five tissue sections were analysed from 3 different controls and 3 hearts each at different time points of GW0742 treatment or physical exercise for five weeks. Heart sections of mice with hereditary cardiomyopathy due to injection of miR 1 in the oocyte<sup>16</sup> served as a positive control.

### *SDS-Page and Western Blot*

Total heart lysates from the mice treated with GW0742 or vehicle alone (DMSO) were prepared, electrophoresed, and blotted as described<sup>16</sup>. Subcellular fractionation of heart tissues was performed using the Qproteome™ Cell Compartment Kit (Quiagen) according to manufacturer's instructions. The following antibodies were used for immunodetection: polyclonal anti-CDK9 antibody from rabbit (H-169, sc-8338, Santa Cruz Biotechnology) in a 1:500 dilution in PBS, 2.5% Blotto, 0.05% Tween-20, polyclonal anti HIF-1 $\alpha$  from goat (Y-15, sc-1254, Santa Cruz Biotechnology) 1:300, polyclonal anti-PECAM-1 from goat (M-20, sc-1506, Santa Cruz Biotechnology) 1:500, polyclonal anti-PPAR $\beta$  from rabbit (H-74, sc-7197, Santa Cruz Biotechnology) 1:500, polyclonal anti CREB from rabbit (kind gift of Dr. M. Montminy, San Diego) 1:2000, polyclonal anti Rho GDI $\alpha$  from rabbit (A-20, sc-360, Santa Cruz Biotechnology) 1:500, polyclonal anti Acetyl-Histone 3 from rabbit (06-599, Upstate, Lake Placid, NY,USA) 1:1000, monoclonal NFATc3 (F-1, sc-8405, Santa Cruz Biotechnology) 1:200, monoclonal anti-HIF-1 $\alpha$  from mouse (MAB 5382, Chemicon) 1:1000, monoclonal anti- $\alpha$ -tubulin from mouse (T6199, Sigma) 1:2000, polyclonal anti- $\beta$ -actin from goat (C-11, sc-1615, Santa Cruz Biotechnology) 1:500, peroxidase-coupled anti-rabbit secondary antibody, peroxidase-coupled anti-mouse secondary antibody, and peroxidase-coupled anti-goat secondary antibody (all diluted 1:2000, Vector Laboratories).

### *Electron microscopy*

For ultrastructural analysis of cardiac muscle, small pieces were fixed in 1.6% glutaraldehyde in 0.1M phosphate buffer pH 7.5 then washed with 0.1M cacodylate buffer pH 7.5 and post-fixed with 1% osmium tetroxide in the same buffer. Samples were embedded in epoxy resin. Thin sections were contrasted with uranyl acetate and lead citrate and

observed with a Philips CM12 electron microscope fitted with a CCD camera (Morada, Olympus SIS).

#### *Cell culture and transient transfection experiments*

Adult cardiomyocytes were isolated using the Adumyts kit (Cellutron) according to manufacturers instructions. Isolated cardiomyocytes were seeded on laminin coated (Invitrogen) chamber slides (Nunc) in serum-containing medium provided in the kit. After 2-3 hours, the medium was replaced by serum-free culture medium. Cardiomyocytes were maintained for 24 hours in serum free medium in the presence of 200nM GW0742 or vehicle. Afterwards, methanol fixed cardiomyocytes were stained with hematoxylin and eosin. Mean cardiomyocyte diameters were determined measuring at least 60 cardiomyocytes per condition from three independent experiments.

Neonatal mouse cardiomyocytes were isolated as described<sup>17</sup> with minor modifications. Briefly, mice at postnatal day 0-1 were sacrificed, the bodies wiped with 70% ethanol, and the hearts excised. Excised hearts were minced with scalpel blades in serum-free DMEM medium (Invitrogen) and tissue fragments transferred to 50 ml Falcon tubes. The supernatant was removed and the tissue incubated with 0.25% Trypsin (Sigma) in serum free DMEM medium at 37°C for 10min. The supernatant containing mostly damaged cells was discarded and replaced by fresh medium containing 0.25% Trypsin. Digestion was carried out in a shaking incubator at 37°C for 20 min, the supernatant collected, and digestion stopped by addition of 50% fetal calf serum (FCS, Lonza). The cells were centrifuged and re-suspended in fresh complete culture medium. Dependent on the remaining tissue peaces, a second and third round of digestion for 20 min each were included. Finally, the cells were pooled, centrifuged, and seeded in 6-well plates in DMEM medium containing 10% FCS, 50 µg/ml gentamycin, and 50 ng/ml amphotericin B.

To investigate the effect of PPAR $\beta$  expression on calcineurin promoter activity, a 2.3 kb fragment of the calcineurin promoter in the pGI3basic luciferase expression vector<sup>18</sup> was co-transfected with PPAR $\beta$  and RxR expression constructs<sup>19</sup>. Neonatal cardiomyocytes at approximately 60% confluence were transfected in 6 well culture plates using Lipofectamine 2000 reagent (Invitrogen). About 0.3 $\mu$ g of the reporter constructs together with 0.1 $\mu$ g of a cytomegalovirus (CMV)-driven  $\beta$ -galactosidase plasmid, and 0.8 $\mu$ g of the expression constructs encoding PPAR $\beta$  and RxR, each were transiently co-transfected and assayed for luciferase- and  $\beta$ -galactosidase activity as described in detail elsewhere<sup>20</sup>. Alternatively, the CnA $\beta$  promoter construct was co-transfected only with the  $\beta$ -galactosidase reporter plasmid and the cells cultured for 48 hours in the presence of 200nM GW0742 or vehicle in the presence or absence of a dominant negative PPAR $\beta$  isoform<sup>19</sup>. The putative PPAR responsive element was deleted from the CnA $\beta$  promoter construct using the Quik Change II site directed mutagenesis kit (Stratagene) with the following oligonucleotides 5'-CATGGGCCTTAGTAGATATGTCGTGTCATACACACAATTC-3' (forward), 5'-GAATTGTGTGTATGACACGACATATCTACTAAGGCCCATG-3' (reverse). This deletion construct was again co-transfected with the PPAR $\beta$  expression construct.

#### *Chromatin immunoprecipitation assay*

Chromatin immunoprecipitation (ChIP) assay was performed on neonatal cardiomyocytes using manufacturers instructions (Upstate). Antibodies (3 $\mu$ g each) against acetylated histone 3 (rabbit polyclonal antibody, 06-599, Upstate), and PPAR $\beta$  (rabbit polyclonal antibody H-74, sc-7197, and goat polyclonal antibody K-20, sc-1987, both Santa Cruz Biotechnology) were used. Normal rabbit serum served as a negative control and a 1:5 and a 1:10 dilution of the input sample as positive control. The histone H3 antibody was used to check for preservation of nucleosomes at the genomic locus. Following

immunoprecipitation, the purified DNA was eluted in 30 $\mu$ l UltraPure DNase, RNase free water (Sigma). For amplification of purified DNA fragments by PCR, 1 $\mu$ l of the diluted input DNA or the immunoprecipitated DNAs were mixed with primers, DNase-free water and Red Taq Ready mix (Sigma). The following primers were used: CnA991 5'-CTGAGTAATAAGATACAGAGGG-3' (forward), CnA1197 5'-TGACTAGTACAGCTTACTCTAGC-3' (backward), Cn3UTRF 5'-CGGCTTCCCAGGGACTCTCACATCT-3' (forward), CnA3UTRB 5'-ATTGCCCCAAGCCCCTTGCT-3' (backward). PCR products were electrophoresed on a 2% agarose gel yielding DNA fragments of 206 bp and 236 bp, respectively.

#### *Electrophoretic mobility shift assays*

The putative PPAR responsive element from the CnA $\beta$  promoter contained the following sequence: 5'-TTGGCCCCTGAACCATTCAACACTGC-3'. The PPAR responsive element from the acyl-CoA oxidase gene (5'-CCCGAACGTGACCTTTGTCCTGGTCC-3') served as positive control. Annealed oligonucleotides were <sup>32</sup>P-end labelled in a T4 polynucleotide kinase reaction (New England Biolabs). PPAR $\beta$  and RxR $\alpha$  proteins were generated from full-length cDNAs in pSG5 vector (Stratagene) using the coupled TNT in-vitro-transcription-translation system (Promega). For supershift assays, the identical antibodies as for the CHIP experiments were used. DNA binding reactions were performed on ice for 30 min with approx. 20ng of proteins in 15  $\mu$ l of a 1x reaction buffer containing 10mM Tris-HCl, pH 7.5, 50mM KCl, 50mM NaCl, 1mM MgCl<sub>2</sub>, 1mM EDTA, 5mM DTT, 5% glycerol, 0.05mg/ml denatured herring sperm DNA. For supershift experiments, the reaction mixes were pre-incubated for 45min with the PPAR $\beta$  antibodies above mentioned prior to addition of the labelled oligonucleotides.

### *Quantitative RT-PCR*

Reverse transcriptase polymerase chain reaction (RT-PCR) was performed with 2 µg of total RNA as described<sup>16</sup>. For qRT-PCR the following primers were used: ANFF 5'-AGGCCATATTGGAGCAAATCCT-3' (forward), ANFB 5'-TGCTTCCTCAGTCTGCTCACT-3' (backward), CnAF 5'-GACCGCGTCGTCAAAGCTG-3' (forward), CnAB 5'-TATGGCAGCACCTCATTGATA-3' (backward), HIF-1F 5'-CCAACCTCAGTGTGGGTACAAG-3' (forward), HIF-1B 5'-GATGAGGAATGGGTTCACAAATC-3' (backward), Myh6F 5'-CGCATCAAGGAGCTCACC-3' (forward), Myh6B 5'-CCTGCAGCCGCATTAAGT-3' (backward), Myh7F 5'-CGCAGCACGAGCTGGATGAG-3' (forward), Myh7B 5'-CGGAGCTGGGTAGCACAAGA-3' (backward), 36B4F 5'-TCCAGGCTTTGGGCATCA-3' (forward), 36B4B 5'-CTTTATCAGCTGCACATCACTCAGA-3' (backward).

### *Echocardiography*

Echocardiography was performed on lightly anesthetized (1% isoflurane in oxygen) mice with a GE Medical System VIVI7 device equipped with an 8- to 14-MHz phased array transducer. The left ventricle (LV) was imaged in parasternal long-axis view to obtain measurements of the LV in time-motion mode. The following measurements were performed: LV end-diastolic diameter (mm/g), interventricular septum diastolic thickness (mm/g), LV posterior wall diastolic thickness (mm/g), and shortening fraction (%). Aortic outflow was estimated by measuring the pulse-wave Doppler velocity in the LV at the level of the aortic annulus and using the following equation:  $\Pi d^2/4 * VTI * HR$ , d is the diameter of the aortic annulus, VTI is the velocity time integral, HR is the heart rate.

### *Statistics*

Data are expressed as means  $\pm$  S.E.M. ANOVA with the Bonferroni test as post hoc test was used vs. control. Differences between two groups were tested using the Mann-Whitney test for non-parametric samples. A p-value less than 0.05 was considered statistically significant.

## Supplementary Legends

### Supplementary Figure 1: PPAR $\beta$ activation induces adult cardiomyocyte growth *in vitro*.

(A) Adult cardiomyocytes were isolated and maintained for 24 hours in serum-free medium in the presence of 200nM GW0742 or vehicle. Mean cardiomyocyte diameters (B) and cardiomyocyte lengths (C) were determined after hematoxylin-eosin staining from at least 60 cells from 3 independent cell preparations for GW0742 or vehicle treatment, respectively. \*\*\* $p < 0.001$ .

### Supplementary Figure 2: The PPAR $\beta$ agonists GW0742 and GW501516 have similar effects on cardiac growth and angiogenesis.

(A) Mean values  $\pm$  S.E.M. of heart to body weight ratios 24 hours after GW0742 or GW501516 injection compared to vehicle-injected controls ( $n=6$  each, \*\* $p < 0.01$ , \*\*\* $p < 0.001$ ). (B) Mean values  $\pm$  S.E.M. of body weights. (C) Mean values  $\pm$  S.E.M. of tibia lengths. (D) High magnifications of heart sections. (E) Mean values  $\pm$  S.E.M. of cardiomyocyte diameters. \*\*\* indicates  $p < 0.001$ . (F) Isolectin B4 staining (brown, DAB substrate) as a marker of vascular cells. (G) Morphometric analysis revealed a similar number of vessels in response to PPAR $\beta$  activation with GW0742 and with GW501516. \*\*\* $p < 0.001$  vs. control. Scale bars: 50  $\mu\text{m}$ .

### Supplementary Figure 3: PPAR $\alpha$ activation does not induce cardiac growth or angiogenesis.

(A) Mean values  $\pm$  S.E.M. of heart to body weight ratios of control mice and animals injected with the PPAR $\alpha$  agonist clofibrate ( $n=4$  each). (B) Mean values  $\pm$  S.E.M. of body weights. (C) High magnifications of heart sections of control mice and animals after clofibrate injection. Scale bars: 50  $\mu\text{m}$ . (D) Mean values  $\pm$  S.E.M. of cardiomyocyte diameters of control mice and animals injected with clofibrate. (E) Isolectin B4 staining as a marker of vascular cells (a-c). Scale bars: 50  $\mu\text{m}$ . (F) Morphometric analysis revealed no difference in the number of vessels in response to PPAR $\alpha$  activation.

**Supplementary Figure 4: Inhibition of adrenergic signalling with propranolol does not influence PPAR $\beta$  induced cardiac growth or angiogenesis.** (A) Mean values  $\pm$  S.E.M. of heart to body weight ratios 24 hours after GW0742, propranolol, or combination of GW0742 and propranolol compared to vehicle-injected controls ( $n=4$  each, \* $p<0.05$ , \*\* $p<0.01$ ). (B) Mean values  $\pm$  S.E.M. of body weights. (C) Mean values  $\pm$  S.E.M. of cardiomyocyte diameters. (D) High magnifications of heart sections. (E) Isolectin B4 staining as a marker of vascular cells. (F) Morphometric analysis revealed a similar number of vessels in response to PPAR $\beta$  activation in the presence or absence of propranolol. \*\*\* $p<0.001$  vs. control. Scale bars: 50  $\mu\text{m}$ .

**Supplementary Figure 5: GW0742 does not significantly alter RNA and protein stability of calcineurin and Hif-1 $\alpha$  in cultured neonatal cardiomyocytes.** RNA and protein stability were assessed indirectly by inhibition of transcription using actinomycin D (5 $\mu\text{g/ml}$ ) or translation inhibition using cycloheximide (80 $\text{mg/ml}$ ) in the presence of GW0742 or vehicle in isolated neonatal cardiomyocytes for the indicated time points ( $n=3$  each). (A) Quantitative RT-PCR analysis of the levels of calcineurin in the presence of GW0742 or vehicle. (B) Western Blot analysis of calcineurin under translation inhibition with cycloheximide in the presence of GW0742 or vehicle.  $\beta$ -actin served as an internal standard. (C) Quantitative RT-PCR analysis of the levels of Hif-1 $\alpha$  under actinomycin treatment in the presence of GW0742 or vehicle. (D) Western Blot analysis of Hif-1 $\alpha$  under translation inhibition with cycloheximide in the presence of GW0742 or vehicle. Note that Hif-1 $\alpha$  protein is barely detectable under control cell culture conditions and disappears completely after cycloheximide treatment.